

Supporting Information

TABLE OF CONTENTS

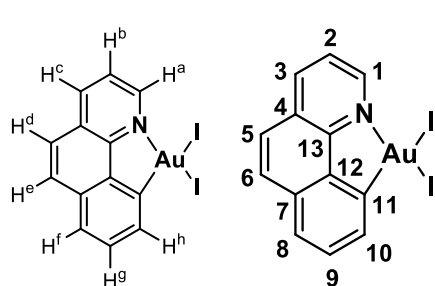
1. Materials and Methods.....	S2
1.1 Materials and instrumentation.....	S2
1.2 Synthesis and characterization of the Au(III) complexes.....	S2
2. Computational Details.....	S6
3. Figures and Tables.....	S8
4. X-ray Crystallography Data.....	S32

1. Materials and Methods

1.1. Materials and instrumentation

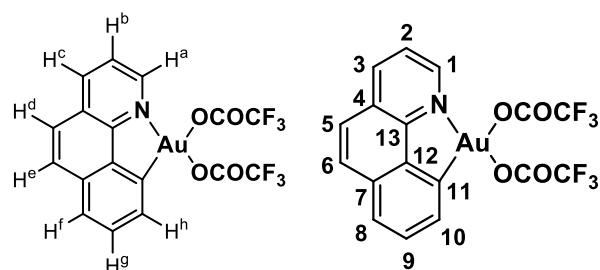
Reagents and solvents used were commercially available reagent quality unless indicated otherwise. *Trans*-ethylene- d_2 was purchased from Cluzeau Info Labo and supplied in a 1 atm lecture bottle (1 atm, 95.2% D). All reactions and manipulations were carried out under an atmosphere of dry argon using standard Schlenk techniques or in a glovebox under inert atmosphere with O_2 and H_2O concentrations < 1.0 ppm. Dry, oxygen-free solvents were employed. Solution 1H , ^{13}C and ^{19}F NMR spectra were recorded on Bruker AVANCE 300, 400 or 500 spectrometers under routine conditions at 298 K unless otherwise specified. The following abbreviations and their combinations are used: br, broad; s, singlet; d, doublet; t, triplet; q, quartet, m, multiplet. The 1H and ^{13}C resonance signals were attributed by means of 2D COSY, HSQC and HMBC experiments. High resolution mass spectra (HRMS) were recorded on a Waters LCT apparatus and/or a Bruker MicrOTOF-Q II TM instrument using ESI or Cryospray ionization sources.

1.2. Synthesis and characterization of the Au(III) complexes



Complex **1** was prepared following a previously described procedure.^[1] To a mixture of gold iodide (194.9 mg, 0.6 mmol) and 10-Iodobenzo[*h*]quinolone **2a-I** (183.7 mg, 0.6 mmol) was added toluene (4 mL) at room temperature and stirred at 60°C for 18h. The resulting suspension was then dried under vacuum and washed with cold DCM to yield **1**

as a red powder (362.3 mg, 96%). 1H -NMR ($CDCl_3$, 400 MHz, 323K) δ , ppm: 10.36 (dd, $J = 5.6$, 1.2 Hz, 1H, H^a), 8.93 (dd, $J = 8.0$, 0.8 Hz, 1H, H^b), 8.55 (dd, $J = 8.0$, 0.4 Hz, 1H, H^c), 7.88 (d, $J = 8.8$ Hz, 1H, H^e), 7.87 (d, $J = 8.0$ Hz, 1H, H^f), 7.79 (dd, $J = 8.0$, 5.6 Hz, 1H, H^b), 7.71 (d, $J = 8.7$ Hz, 1H, H^d), 7.59 (t, $J = 8.0$ Hz, 1H, H^g); $^{13}C\{^1H\}$ -NMR ($CDCl_3$, 100 MHz, 323K) δ , ppm: 154.81 (C13), 153.63 (C11), 150.00 (C1), 140.64 (C12), 140.26 (C3), 135.88 (C7), 134.52 (C10), 131.44 (C9), 130.38 (C6), 129.22 (C4), 126.33 (C8), 124.06 (C5), 122.60 (C2).

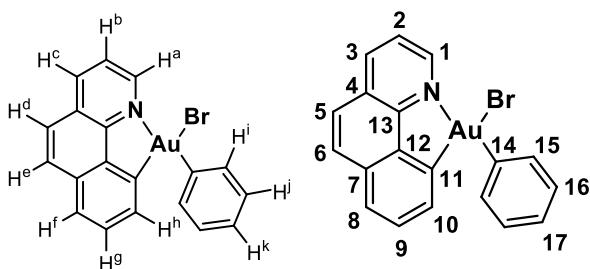


2: Complex **1** (248.1 mg, 0.39mmol) and $AgOAc^F$ (183.3 mg, 0.83mmol) were suspended in CH_2Cl_2 (8 mL). After stirring for 10 min at room temperature, solvent was removed under vacuum and acetone (8 mL) was added. The resulting light yellow mixture

was filtered through *Celite*®, dried under vacuum and washed with hexanes (3 x 3 mL) to give the

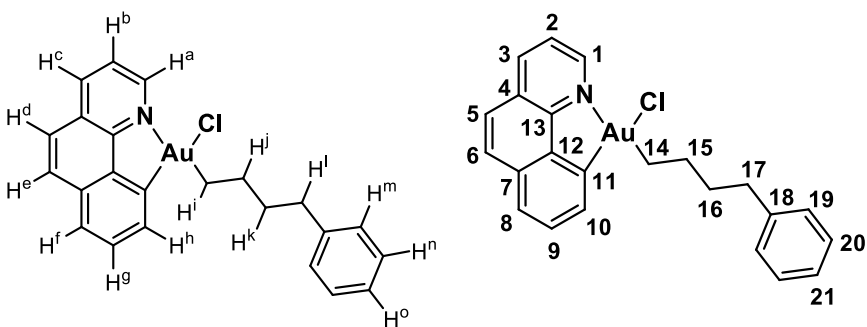
¹ J. Serra, T. Parella, X. Ribas, *Chem. Sci.* **2017**, *8*, 946.

desired complex as a pale yellow solid (213.4 mg, 91%). **¹H-NMR** (acetone-*d*₆, 400 MHz, 298K) δ , ppm: 9.08 (dd, $J = 8.0, 1.2$ Hz, 1H, H^c), 8.95 (dd, $J = 5.6, 1.2$ Hz, 1H, H^a), 8.16 (dd, $J = 8.0, 5.6$ Hz, 1H, H^b), 8.10 (m, 3H, H^d+H^e+H^f), 7.72 (t, $J = 8.0$ Hz, 1H, H^g), 7.25 (d, $J = 7.6$ Hz, 1H, H^h); **¹³C{¹H}-NMR** (acetone-*d*₆, 100 MHz, 298K) δ , ppm: 153.32 (C13), 148.15 (C1), 143.44 (C3), 140.54 (C11), 137.18 (C12), 135.52 (C7), 130.22 (C9), 129.60 (C5), 129.35 (C4), 128.29 (C8), 126.22 (C10), 125.50 (C6), 124.08 (C4); **¹⁹F{¹H}-NMR** (acetone-*d*₆, 282 MHz, 298K) δ , ppm: -74.85 (s, CF₃*trans* to N, 3F), -73.99 (s, br, CF₃*cis* to N, 3F); **HRMS (ESI)** (Acetone/CH₃CN, *m/z*): calcd for C₁₇H₈AuF₆NO₄ [M+Na]⁺ 623.9915, found: 623.9962.



3-Br: To a solution of complex **2** (210.5 mg, 0.35 mmol) in THF (10 mL) was added dropwise PhMgBr (2.1 equiv, 2M in diethyl ether) at -78°C. The reaction mixture was stirred at -78°C for 1 h and then at room temperature for 1 h. The solvent was

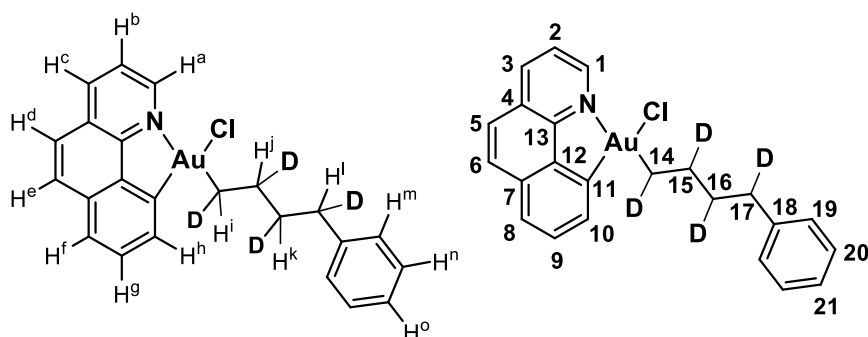
removed in vacuo and the resulting solid was dissolved in CH₂Cl₂ (8 mL) and washed with distilled water (2 x 2 mL). The organic phase was dried over Na₂SO₄, filtered through *Celite*® and all volatiles were then removed under vacuum to give a pale yellow solid, which was finally purified by column chromatography on silica gel (CH₂Cl₂:hexane 3:2) to yield **3-Br** as a white solid (110.0 mg, 59%). **¹H-NMR** (CDCl₃, 500 MHz, 298K) δ , ppm: 9.89 (dd, $J = 5.0, 1.5$ Hz, 1H, H^a), 8.53 (dd, $J = 8.0, 1.5$ Hz, 1H, H^c), 7.93 (d, $J = 8.5$ Hz, 1H, H^e), 7.85 (dd, $J = 8.0, 5.0$ Hz, 1H, H^b), 7.83 (dd, $J = 7.5, 0.5$ Hz, 1H, H^f), 7.78 (d, $J = 8.5$ Hz, 1H, H^d), 7.61 (dd, $J = 8.0, 1.0$ Hz, 2H, Hⁱ), 7.54 (t, $J = 7.5$ Hz, 1H, H^g), 7.31 (t, $J = 7.5$ Hz, 2H, H^j), 7.25 (tt, $J = 7.5, 1.5$ Hz, 1H, H^k), 7.06 (dd, $J = 7.5, 1.0$ Hz, 1H, H^h); **¹³C{¹H}-NMR** (CDCl₃, 125 MHz, 298K) δ , ppm: 151.97 (C13), 149.41 (C11), 148.68 (C1), 141.18 (C14), 139.56 (C3), 138.60 (C7), 134.50 (C12), 133.08 (C15), 131.66 (C10), 130.44 (C9), 129.70 (C6), 129.44 (C16), 127.77 (C4), 126.21 (C8), 125.97 (C17), 124.11 (C5), 122.91 (C2); **HRMS (ESI)** (CHCl₃, *m/z*): calcd for C₁₉H₁₃AuN [M⁺] 452.0714, found: 452.0722. **Anal. Calcd for C₁₉H₁₃AuBrN:** C, 42.88; H, 2.46; N, 2.63. Found: C, 42.91; H, 2.34; N, 2.98.



5A-Cl: In an inert-atmosphere glovebox, a pressure screw-cap NMR tube was charged with **3-Br** (16.0 mg, 0.03 mmol) in CD₂Cl₂

(0.35 mL). AgSbF₆ (12.4 mg, 0.036 mmol) was placed into a small glass vial and solubilized in

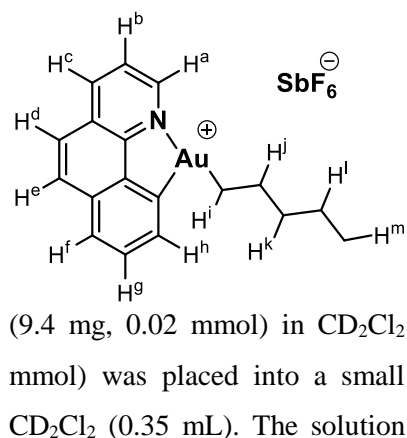
CD₂Cl₂ (0.35 mL). The solution was loaded into a plastic syringe equipped with a stainless steel needle, and the syringe was closed by blocking the needle with a septum. Outside the glovebox, the NMR tube was pressurized under argon atmosphere and cooled down to -60 °C (Acetone/N₂coldbath). At this temperature, the solution of AgSbF₆ was added. The overall mixture was degassed 3 times using the Freeze-Pump-Thaw degassing technique and 2 bar of ethylene were added. The reaction was monitored by ¹H-NMR. After heating overnight at 40°C the ethylene pressure was released and the reaction crude was filtered through *Celite*® on a vial-containing *n*Bu₄N-Cl (10.0 mg, 0.036 mmol). The resulting solution was purified by column chromatography on silica gel (CH₂Cl₂:hexane 2:1) to give **5A-Cl** as a white solid (9.6 mg, 60%). ¹H-NMR (CDCl₃, 400 MHz, 298K) δ, ppm: 9.58 (dd, *J* = 5.2, 1.6 Hz, 1H, H^a), 8.46 (dd, *J* = 8.0, 1.6 Hz, 1H, H^c), 7.92 (d, *J* = 8.8 Hz, 1H, H^d), 7.86 (dd, *J* = 7.6, 0.8 Hz, 1H, H^f), 7.82 (m, 2H, H^b + H^h), 7.75 (d, *J* = 8.8 Hz, 1H, H^e), 7.74 (t, *J* = 7.6 Hz, 1H, H^g), 7.26 (m, 4H, H^m + Hⁿ), 7.18 (tt, *J* = 7.2, 1.6 Hz, 1H, H^o), 2.76 (t, *J* = 8.0 Hz, 2H, H^l), 2.72 (t, *J* = 8.0 Hz, 2H, Hⁱ), 1.97 (m, 4H, H^j + H^k); ¹³C{¹H}-NMR (CDCl₃, 100 MHz, 298K) δ, ppm: 150.81 (C13), 147.00 (C1), 145.37 (C11), 142.70 (C18), 139.20 (C7), 139.08 (C3), 134.71 (C12), 130.22 (C9), 129.56 (C5), 128.51 (C19), 128.23 (C20), 128.13 (C10), 127.41 (C4), 126.22 (C8), 125.57 (C21), 124.07 (C6), 122.73 (C2), 35.78 (C17), 34.24 (C14), 34.13 (C15), 30.84 (C16); HRMS (ESI) (CHCl₃, *m/z*): calcd for C₂₃H₂₁AuN [M⁺] 508.1340, found: 508.1346; Anal. Calcd for C₂₃H₂₁AuNCl: C, 50.80; H, 3.89; N, 2.58. Found: C, 50.45; H, 3.48; N, 2.89.



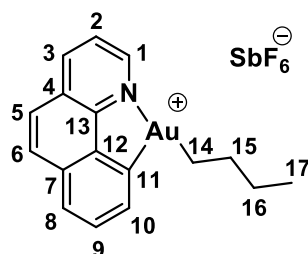
5A-Cl-d₄: In an inert-atmosphere glovebox, a pressure screw-cap NMR tube was charged with **3-Br** (14.6 mg, 0.027 mmol) in CD₂Cl₂

(0.3mL). AgSbF₆ (12.0mg, 0.035 mmol) was placed into a small glass vial and solubilized in CD₂Cl₂ (0.3 mL). The solution was loaded into a plastic syringe equipped with a stainless steel needle, and the syringe was closed by blocking the needle with a septum. Outside the glovebox, the NMR tube was filled with argon and cooled down to -60 °C (Acetone/N₂ coldbath). At this temperature, the solution of AgSbF₆ was added. The overall mixture was degassed 3 times using the Freeze-Pump-Thaw degassing technique and 1 bar of *trans*-ethylene-*d*₂ was added. After heating for 24 h at 40°C, the NMR tube was refilled with 1 bar of *trans*-ethylene-*d*₂ and the mixture was heated for 24 h more at 40°C. Then, in an inert-atmosphere glovebox, the reaction crude was filtered through *Celite*® on a vial-containing *n*Bu₄NCl (9.2 mg, 0.033 mmol). The resulting solution was analyzed by NMR without further purification. **5A-Cl-d₄** was isolated as a white solid (5.0 mg,

33%) by column chromatography on silica gel (CH₂Cl₂:hexane 2:1). **¹H-NMR** (CD₂Cl₂, 500 MHz, 298K) δ, ppm: 9.43 (dd, *J* = 5.1, 1.5 Hz, 1H, H^a), 8.45 (dd, *J* = 8.0, 1.5 Hz, 1H, H^c), 7.88 (d, *J* = 8.8 Hz, 1H, H^d), 7.83 (dd, *J* = 7.9, 0.8 Hz, 1H, H^f), 7.80 – 7.67 (m, 4H, H^b + H^h + H^e + H^g), 7.27 – 7.19 (m, 4H, H^m + Hⁿ), 7.15 (tt, *J* = 7.2, 1.6 Hz, 1H, H^o), 2.69 (d, *J* = 6.1 Hz, 1H, H^l), 2.59 (d, *J* = 5.7 Hz, 1H, Hⁱ), 1.88 (t, *J* = 7.0 Hz, 1H, H^j or H^k), 1.84 (t, *J* = 7.0 Hz, 1H, H^j or H^k); **¹³C{¹H}-NMR** (CD₂Cl₂, 125 MHz, 298K) δ, ppm: 151.18 (C13), 147.29 (C1), 145.77 (C11), 143.38 (C18), 139.83 (C3), 139.58 (C7), 135.19 (C12), 130.62 (C9), 129.93 (C5), 128.98 (C19), 128.72 (C20), 128.48 (C10), 127.99 (C4), 126.72 (C8), 126.07 (C21), 124.76 (C6), 123.39 (C2), 35.77 (t, C17), 34.23 (t,

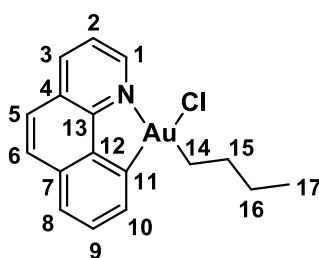
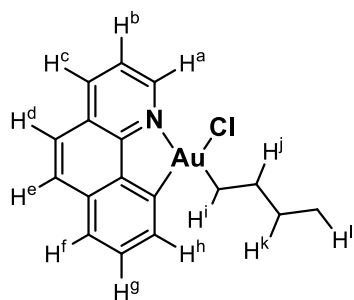


C14), 33.67 (t, C15), 30.73 (t, C16); **HRMS (ESI)** (CHCl₃, *m/z*): calcd for C₂₃H₁₇D₄AuN [M⁺] 512.1591, found: 512.1559.



6A: In an inert-atmosphere glovebox, a pressure screw-cap NMR tube was charged with **6-Cl** (0.35 mL). AgSbF₆ (8.2 mg, 0.024 mmol) was solubilized also in CD₂Cl₂ and the solution was loaded into a plastic syringe

equipped with a stainless steel needle, and the syringe was closed by blocking the needle with a septum. Outside the glovebox, the NMR tube was pressurized under argon atmosphere and cooled down to –60 °C (Acetone/N₂coldbath). At this temperature, the solution of AgSbF₆ was added. The tube was immediately introduced in the NMR machine and the reaction was monitored by ¹H-NMR from -60°C to room temperature. Complex **6A** was generated at -60°C and no formation of butane or 2-butenes was observed upon warming. The complex was characterized at room temperature: **¹H-NMR** (CD₂Cl₂, 400 MHz, 298K) δ, ppm: 8.98 (dd, *J* = 3.6 Hz, 1H, H^a), 8.63 (dd, *J* = 8.0 Hz, 1H, H^c) 8.00 (m, 3H, H^b + H^e + H^f), 7.89 (d, *J* = 8.8 Hz, 1H, H^d), 7.79 (m, 2H, H^h+H^g), 2.58 (dd, *J* = 7.6 Hz, 2H, Hⁱ), 1.88 (dd, *J* = 7.6 Hz, 2H, H^j), 1.65 (sext, *J* = 7.6 Hz, 2H, H^k), 1.07 (t, *J* = 7.6 Hz, 3H, H^l); **¹³C{¹H}-NMR** (CD₂Cl₂, 100 MHz, 298K) δ, ppm: 147.79 (C13), 146.59 (C1), 140.57 (C3), 135.04 (C7), 133.76 (C11), 131.64 (C12), 130.24 (C9), 129.47 (C6), 128.71 (C10), 128.00 (C8), 125.39 (C4), 124.76 (C5), 123.99 (C2), 38.86 (C14), 32.43 (C15), 25.36 (C16), 13.64 (C17); **HRMS (ESI)** (CH₂Cl₂, *m/z*): calcd for C₁₇H₁₇AuN [M⁺] 432.1021, found: 432.1027.



6-Cl: To a solution of complex **2** (41.9 mg, 0.07 mmol) in THF (4 mL) was added dropwise BuMgCl (2.1 equiv, 2M in diethyl ether) at -78°C. The reaction mixture was stirred at -78°C for 1 h and then at room

temperature for 1 h. The solvent was removed in vacuo and the resulting solid was dissolved in CH₂Cl₂ (3 mL) and washed with distilled water (2 x 1 mL). The collected organic phases were dried over Na₂SO₄, filtered through *Celite*® and all volatiles were then removed under vacuum to give the light yellow solid, which was subsequently purified by column chromatography on silica gel (CH₂Cl₂:hexane 3:1) to yield **6-Cl** as a white solid (23.9 mg, 73%). ¹H-NMR (CDCl₃, 400 MHz, 298K) δ, ppm: 9.58 (dd, *J* = 5.2, 1.2 Hz, 1H, H^a), 8.46 (dd, *J* = 8.0, 1.2 Hz, 1H, H^c), 7.92 (d, *J* = 8.8 Hz, 1H, H^e), 7.88 (m, 2H, H^g + H^f), 7.81 (dd, *J* = 8.0, 5.2 Hz, 1H, H^b), 7.76 (m, 2H, H^h + H^d), 2.71 (t, *J* = 7.6 Hz, 2H, Hⁱ), 1.92 (quint, *J* = 7.6 Hz, 2H, H^j), 1.63 (sext, *J* = 7.6 Hz, 2H, H^k), 1.03 (t, *J* = 7.6 Hz, 3H, H^l); ¹³C{¹H}-NMR (CDCl₃, 100 MHz, 298K) δ, ppm: 150.76 (C13), 146.96 (C1), 145.37 (C11), 139.20 (C7), 139.02 (C3), 134.68 (C4), 130.18 (C10), 129.55 (C6), 128.14 (C9), 127.38 (C12), 126.19 (C8), 124.05 (C5), 122.71 (C2), 34.71 (C14), 33.40 (C15), 25.68 (C16), 14.06 (C17); HRMS (ESI) (CHCl₃, *m/z*): calcd for C₁₇H₁₇AuN [M⁺] 432.1021, found: 432.1018.

2. Computational Details

All calculations were performed using the Gaussian 09 package^[2] and the B3PW91 hybrid^[3] functional on the real cationic experimental systems, taking into account solvent effect (dichloromethane) by means of polarizable continuum model PCM.^[4] The weakly coordinating counter-anion SbF₆⁻ has not been considered in the calculations since we previously showed that even a more coordinating counter-anion like NTf₂⁻ has no significant impact on the reaction profile (migratory insertion, β-hydride elimination) in similar processes than those described in this work.^[5] The gold atom was described with the relativistic electron core potential SDD and associated basis set,^[6] augmented by a set of f-orbital polarization functions.^[7] The 6-31G** basis set were employed for other atoms. All stationary points involved were fully optimized in solvent.

² Gaussian 09, Revision C.01, M. J. Frisch, G. W. Trucks, H. B. Schlegel, G. E. Scuseria, M. A. Robb, J. R. Cheeseman, G. Scalmani, V. Barone, B. Mennucci, G. A. Petersson, H. Nakatsuji, M. Caricato, X. Li, H. P. Hratchian, A. F. Izmaylov, J. Bloino, G. Zheng, J. L. Sonnenberg, M. Hada, M. Ehara, K. Toyota, R. Fukuda, J. Hasegawa, M. Ishida, T. Nakajima, Y. Honda, O. Kitao, H. Nakai, T. Vreven, J. A. Montgomery, Jr., J. E. Peralta, F. Ogliaro, M. Bearpark, J. J. Heyd, E. Brothers, K. N. Kudin, V. N. Staroverov, T. Keith, R. Kobayashi, J. Normand, K. Raghavachari, A. Rendell, J. C. Burant, S. S. Iyengar, J. Tomasi, M. Cossi, N. Rega, J. M. Millam, M. Klene, J. E. Knox, J. B. Cross, V. Bakken, C. Adamo, J. Jaramillo, R. Gomperts, R. E. Stratmann, O. Yazyev, A. J. Austin, R. Cammi, C. Pomelli, J. W. Ochterski, R. L. Martin, K. Morokuma, V. G. Zakrzewski, G. A. Voth, P. Salvador, J. J. Dannenberg, S. Dapprich, A. D. Daniels, O. Farkas, J. B. Foresman, J. V. Ortiz, J. Cioslowski, and D. J. Fox, Gaussian, Inc., Wallingford CT, **2009**.

³ (a) A. D. Becke *J. Chem. Phys.* **1993**, *98*, 5648; (b) J. P. Perdew, in *Electronic Structure of Solids '91*, Ed. P. Ziesche and H. Eschrig, Akademie Verlag, Berlin, **1991**, 11.

⁴ J. Tomasi, B. Mennucci, R. Cammi, *Chem. Rev.* **2005**, *105*, 2999.

⁵ F. Rekhroukh, L. Estévez, S. Mallet-Ladeira, K. Miqueu, A. Amgoune, D. Bourissou, *J. Am. Chem. Soc.* **2016**, *138*, 11920.

⁶ D. Andrae, U. Häussermann, M. Dolg, H. Stoll, H. Preuss, *Theor. Chim. Acta* **1990**, *77*, 123.

⁷ A. W. Ehlers, M. Bihme, S. Dapprich, A. Gobbi, A. Hijllwarth, V. Jonas, K. F. Kiihler, R. Stegmann, A. Veldkamp, G. Frenking, *Chem. Phys. Letters* **1993**, *208*, 111.

Frequency calculations were undertaken to confirm the nature of the stationary points, yielding one imaginary frequency for transition states (TS), corresponding to the expected process, and all of them positive for *minima*. The connectivity of the transition states and their adjacent *minima* was confirmed by intrinsic reaction coordinate (IRC)^[8] calculations.

Natural Bond Orbital^[9] calculations (NBO, 5.9 version)^[10] have been carried to analyze the bonding situation, in particular for the description of gold π -complexes and complexes involving β -H and γ -H interactions. Natural Localized Molecular Orbital (NLMO) were plotted with Molekel 4.3^[11] and all the geometrical structures with Gaussview 5.0^[12] and CYLview.^[13]

¹³C NMR chemical shifts for complex **4** (*cis* and *trans* isomers) were evaluated by employing the direct implementation of the Gauge Including Atomic Orbitals (GIAO),^[14] with the IGLOII^[15] basis set on C, H and N atoms, using as reference the corresponding SiMe₄ shielding constant calculated at the same level of theory.

Bader^[16] charges have been computed for the dicationic species [(N,C)Au]²⁺ and [(P,C)Au]²⁺ in order to analyze atomic charge at gold.

⁸ (a) K. Fukui, *Acc. Chem. Res.*, **1981**, *14*,363; (b) H. P. Hratchian, H. B. Schlegel, in *Theory and Applications of Computational Chemistry: The First 40 Years*, Ed. C. E. Dykstra, G. Frenking, K. S. Kim, G. Scuseria, Elsevier, Amsterdam, **2005**, 195.

⁹(a) E. Reed, L. A. Curtiss, F. Weinhold, *Chem. Rev.* **1988**, *88*, 899; (b) J. P. Foster F. Weinhold, *J. Am. Chem. Soc.* **1980**, *102*, 7211; (c) A. E. Reed, F. Weinhold, *J. Chem. Phys.* **1985**, *83*, 1736.

¹⁰NBO 5.0 program, E. D. Glendening, J. K. Badenhoop, A. E. Reed, J. E. Carpenter, J. A. Bohmann, C. M. Morales, F. Weinhold, Theoretical Chemistry Institute, University of Wisconsin, Madison, **2001**.

¹¹ MOLEKEL 4.3, P. Flükiger, H. P. Lüthi, S. Portmann, J. Weber, Swiss Center for Scientific Computing, Manno (Switzerland), **2000-2002**.

¹² GaussView, Version 5, R. Dennington, T. Keith, J. Millam, *Semichem Inc.*, Shawnee Mission, KS, **2009**.

¹³ C.Y. Legault, CYLview, 1.0b, Université de Sherbrooke, **2009** (<http://www.cylview.org>).

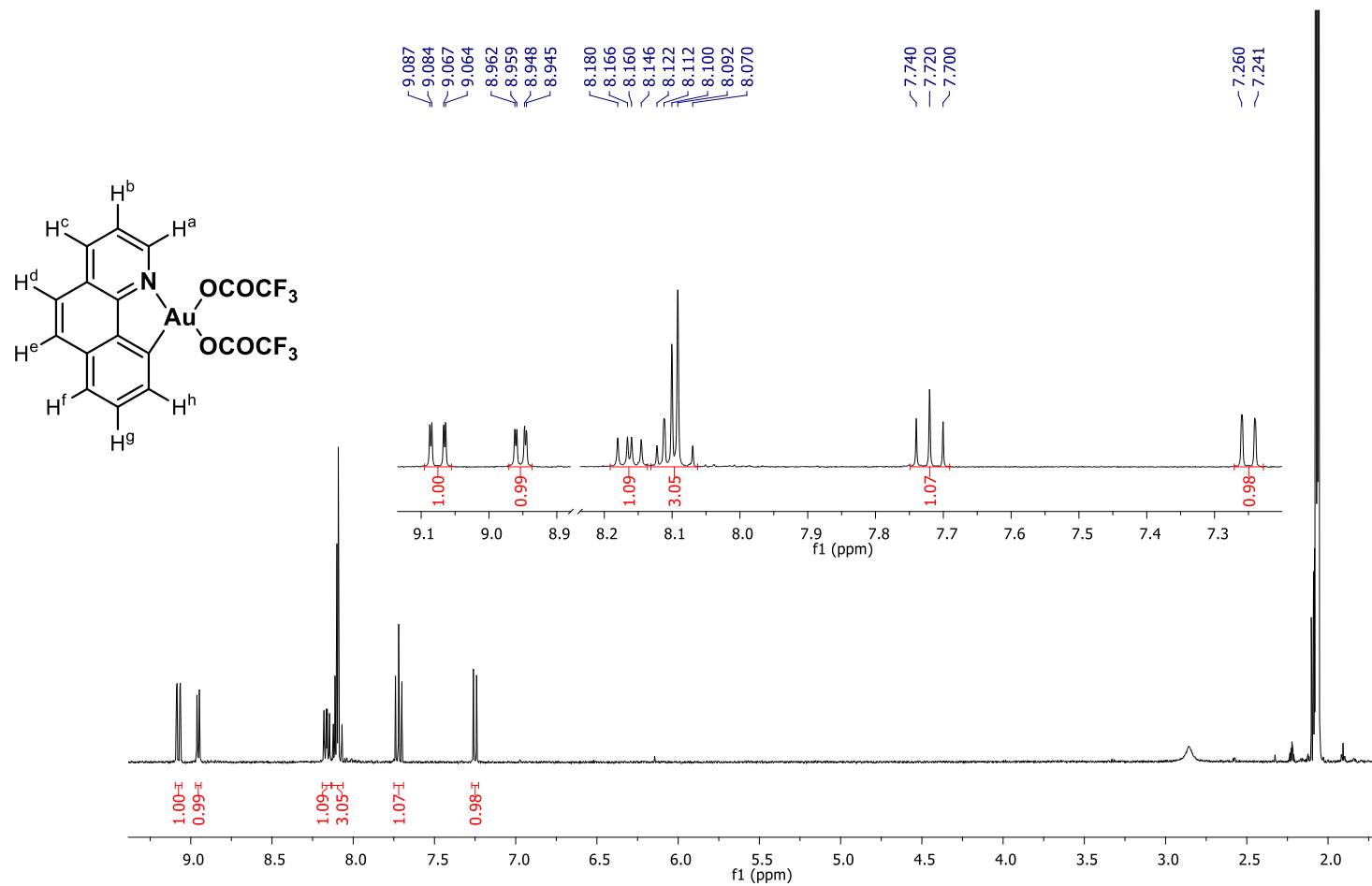
¹⁴ (a) F. London, *J. Phys. Radium* **1937**, *8*, 397; (b) R. McWeeny, *Phys. Rev.* **1962**, *126*, 1028; (c) R. Ditchfield, *Mol. Phys.* **1974**, *27*, 789; (d) K. Wolinski, J. F. Hilton, P. Pulay, *J. Am. Chem. Soc.* **1990**, *112*, 8251; (e) J. R. Cheeseman, G. W. Trucks, T. A. Keith, M. J. Frisch, *J. Chem. Phys.* **1996**, *104*, 5497.

¹⁵ W. Kutzelnigg, U. Fleischer, M. Schindler, *The IGLO-Method: Ab Initio Calculation and Interpretation of NMR Chemical Shifts and Magnetic Susceptibilities*, Springer-Verlag, Heidelberg, **1990**, vol. 23.

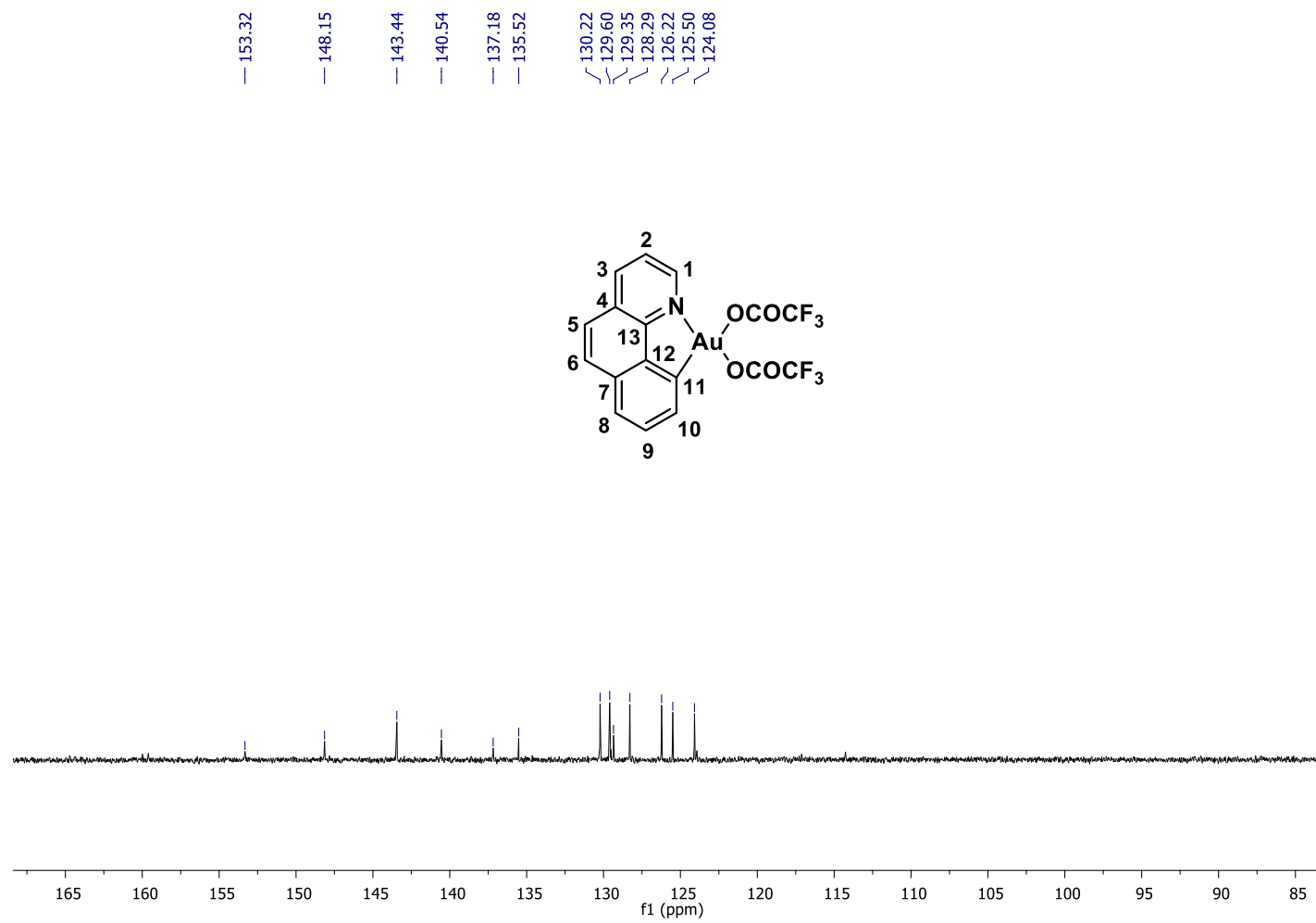
¹⁶ (a) R. F. W. Bader, *Atoms in Molecules: A Quantum Theory*; Oxford University Press: New-York Ed., **1990**; (b) R. F. W. Bader, *Chem. Rev.* **1991**, *91*, 893; (c) AIMAll (Version 10.10.11), Todd A. Keith, **2010** (aim.tkgristmill.com).

3. Figures and Tables

Figure S1. a) ^1H -NMR spectrum of complex **2** in acetone- d_6 , 400 MHz, 298 K; b) $^{13}\text{C}\{^1\text{H}\}$ -NMR spectrum (acetone- d_6 , 100 MHz, 298 K); c) $^{19}\text{F}\{^1\text{H}\}$ -NMR spectrum (acetone- d_6 , 282 MHz, 298 K).



b)



c)

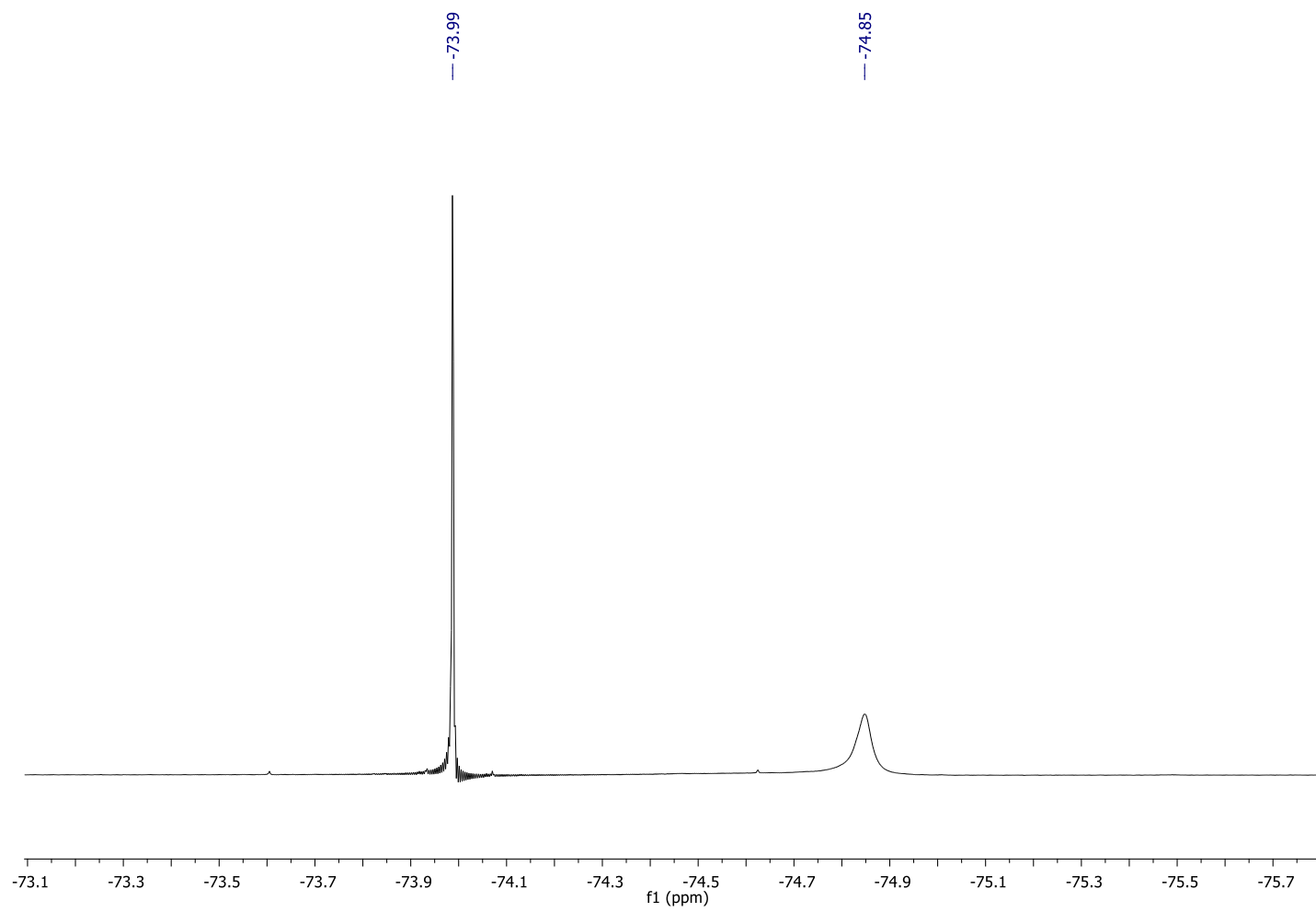
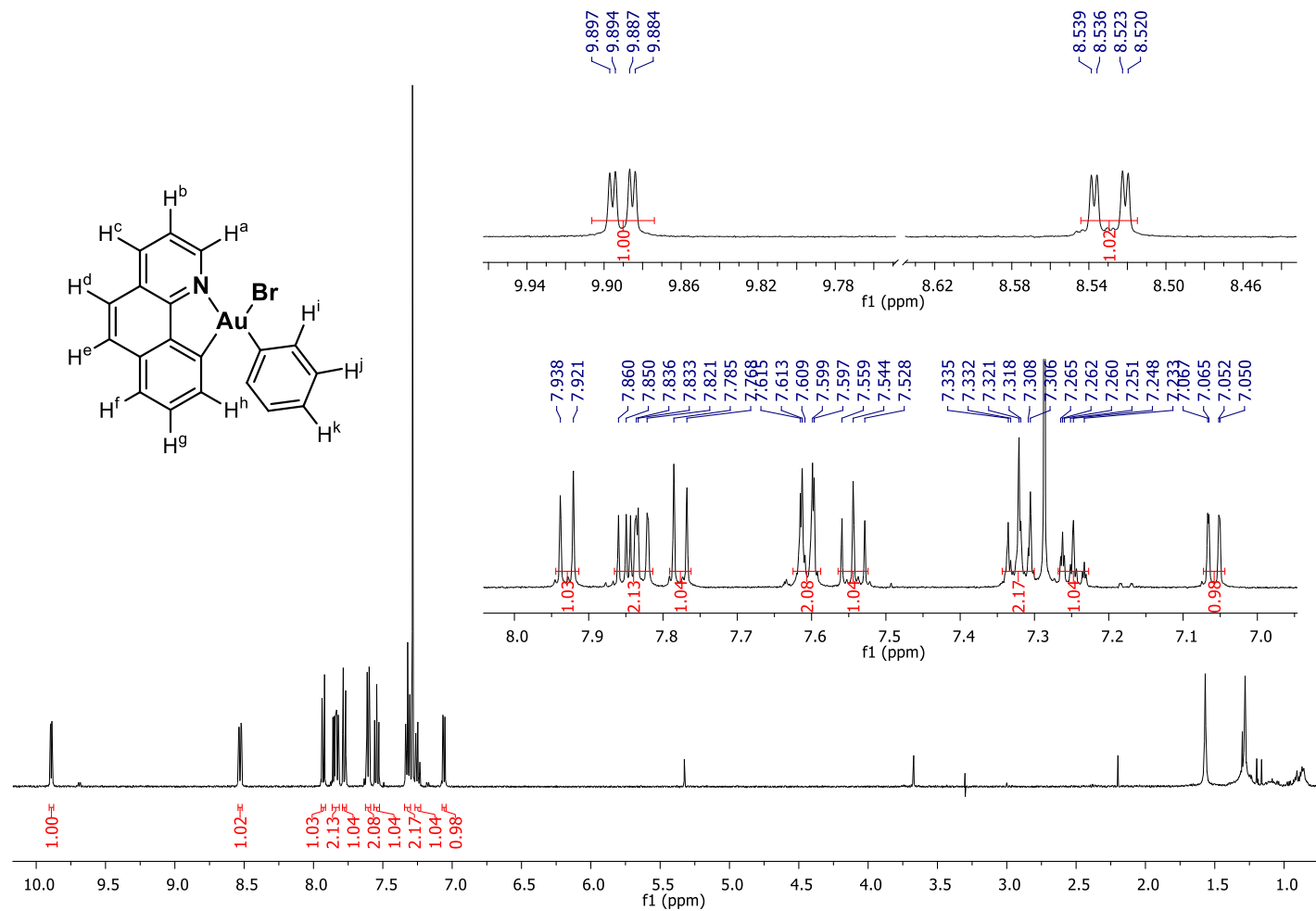


Figure S2. a) ^1H -NMR spectrum of complex **3-Br** in CDCl_3 , 500 MHz, at 298 K; b) $^{13}\text{C}\{^1\text{H}\}$ -NMR spectrum (CDCl_3 , 125 MHz, 298 K).

a)



b)

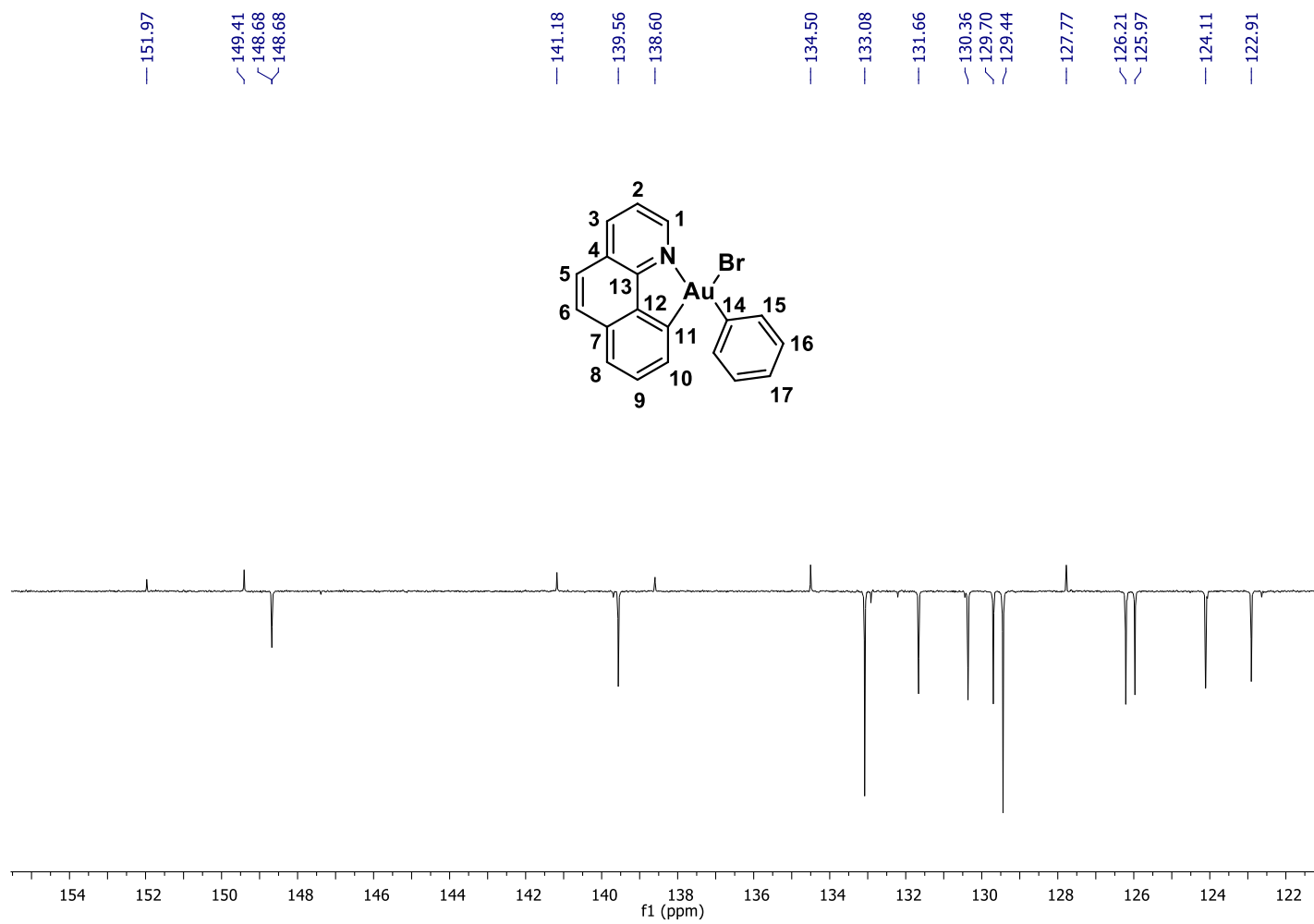
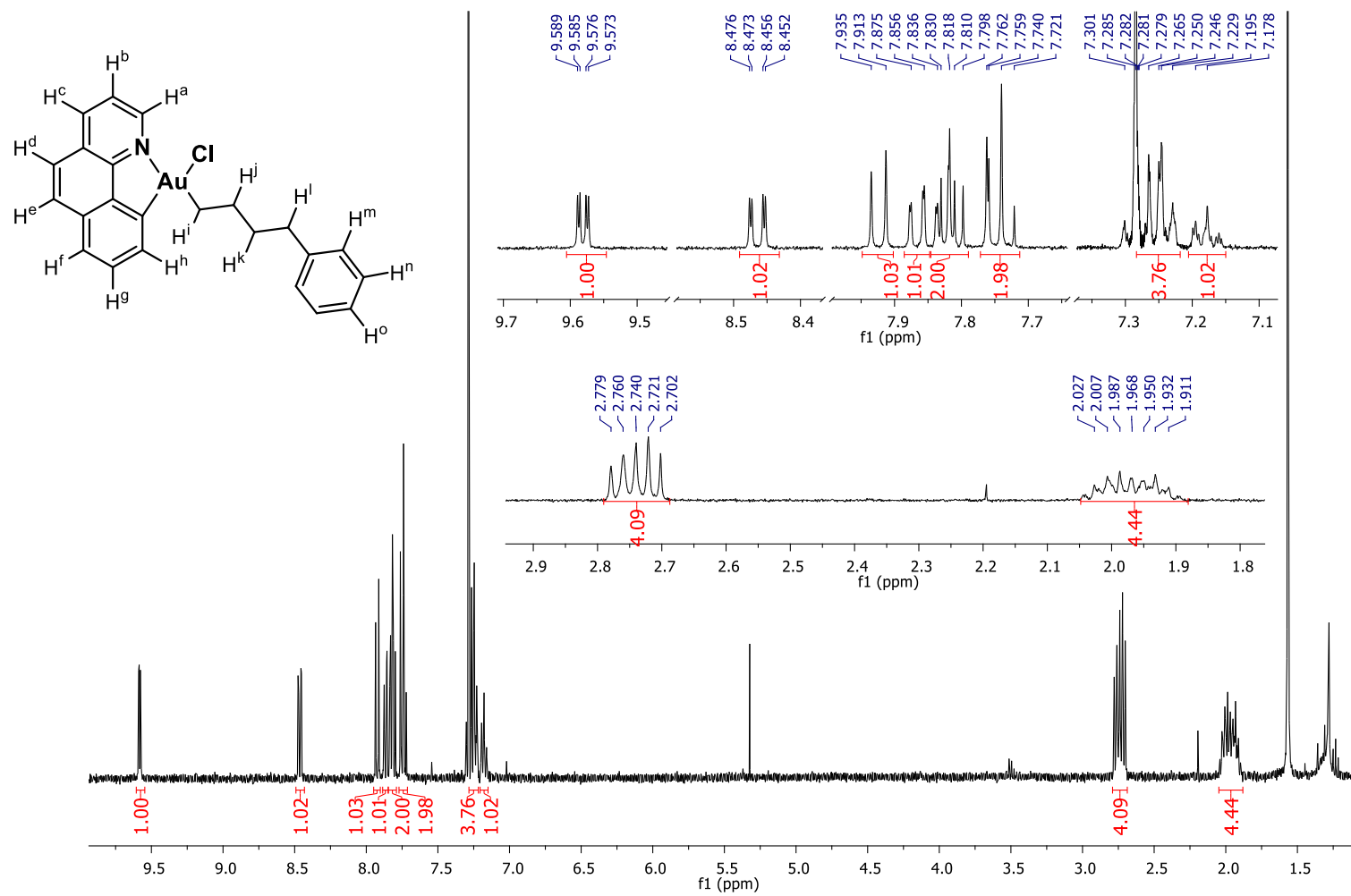


Figure S3. a) ^1H -NMR spectrum of complex **5A-Cl** in CDCl_3 , 400 MHz, at 298 K; b) $^{13}\text{C}\{^1\text{H}\}$ -NMR spectrum (CDCl_3 , 100 MHz, 298 K).

a)



b)

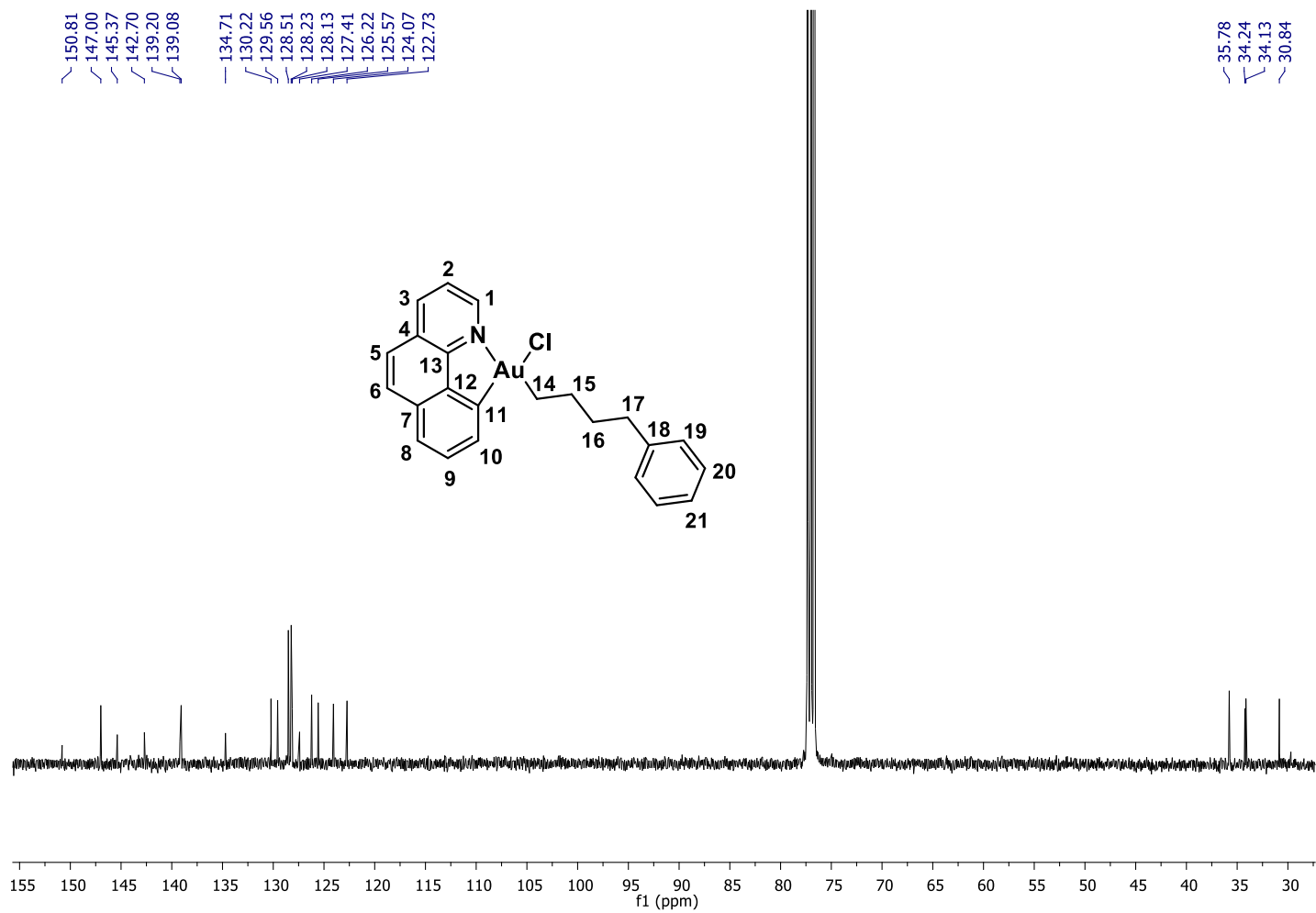
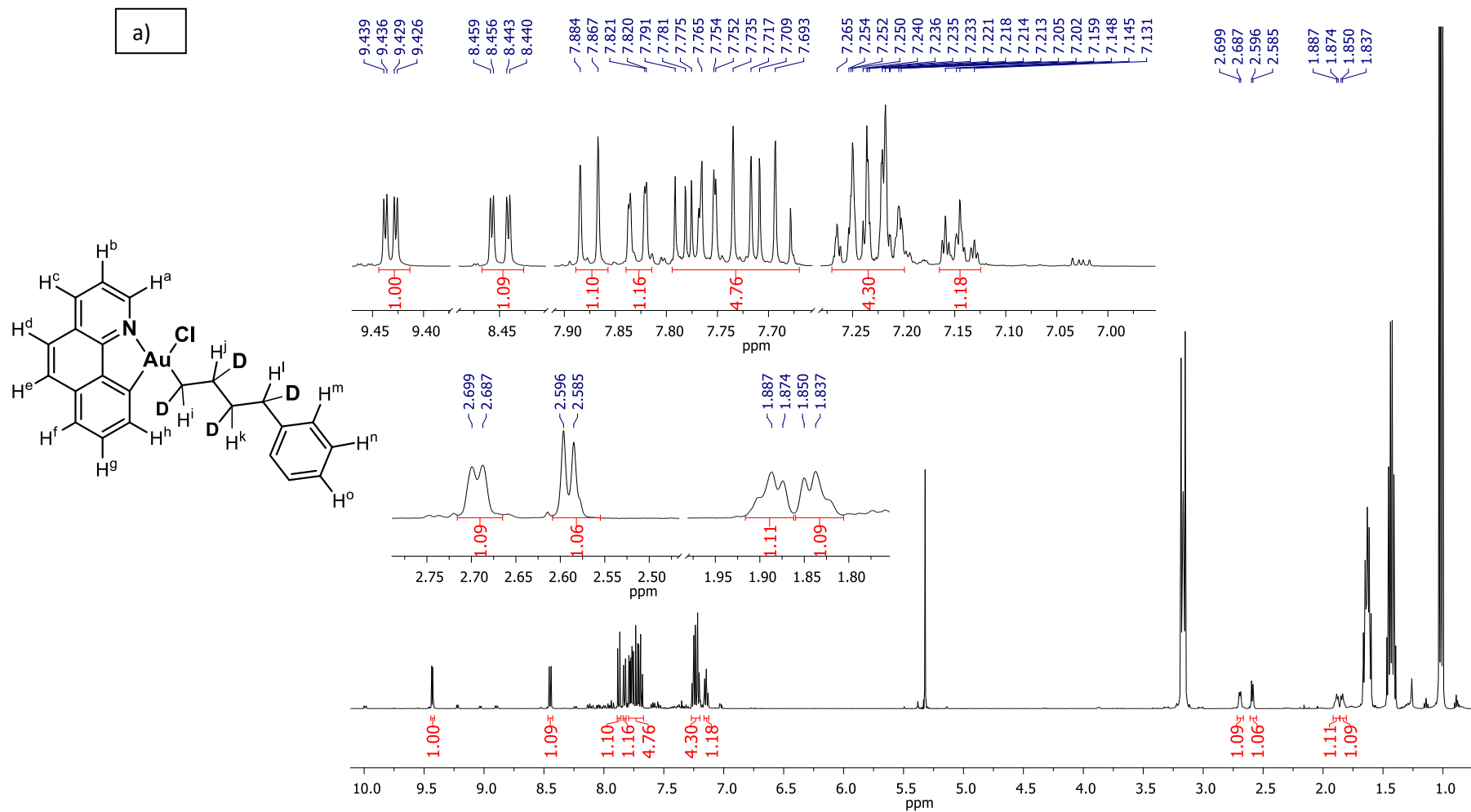
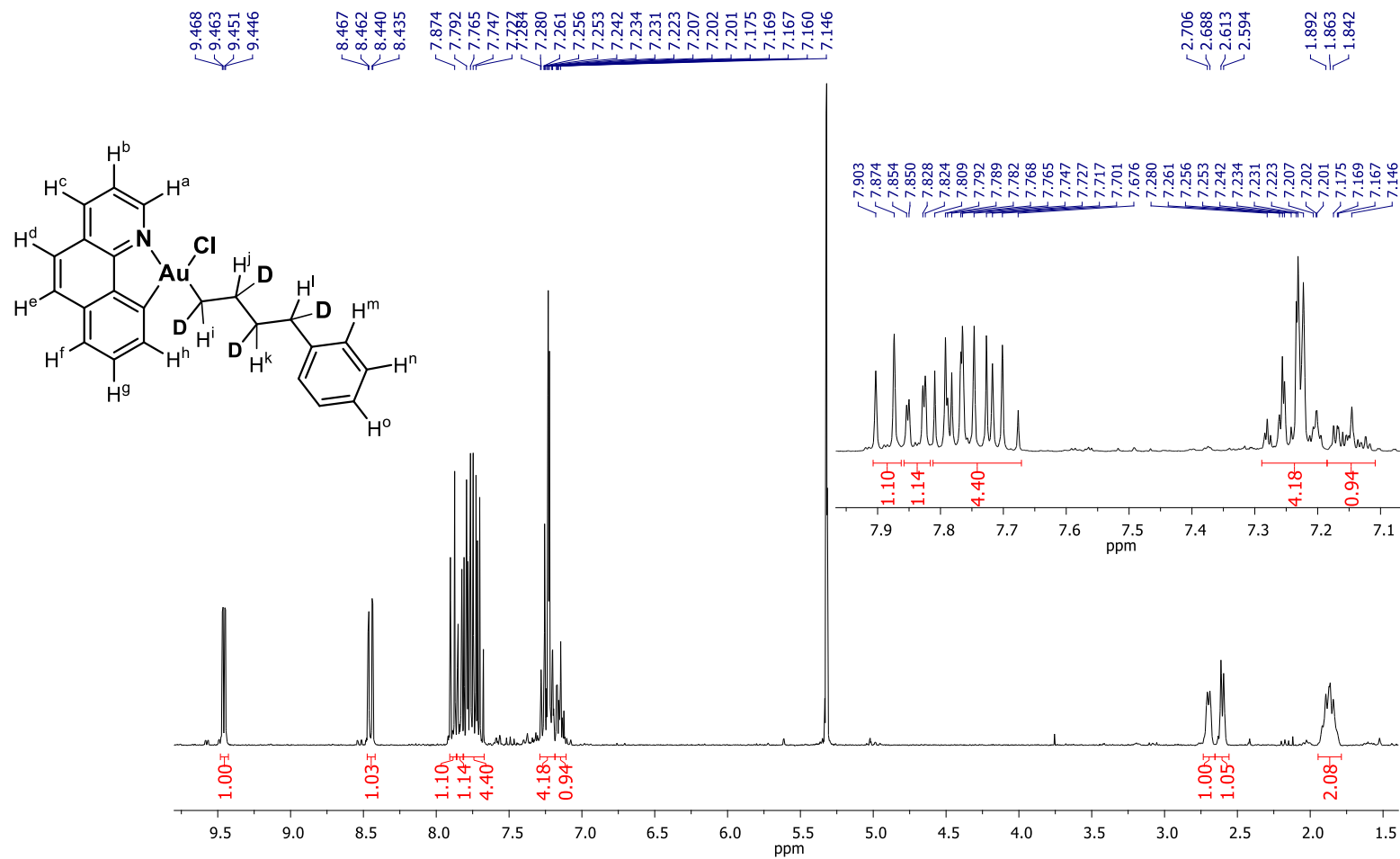


Figure S4. a) ^1H -NMR spectrum of complex **5A-Cl-*d*₄** in CD_2Cl_2 , 500 MHz, at 298 K (crude); b) ^1H -NMR spectrum of complex **5A-Cl-*d*₄** in CD_2Cl_2 , 300 MHz, at 298 K (purified) ; c) $^{13}\text{C}\{^1\text{H}\}$ -NMR spectrum in CD_2Cl_2 , 125 MHz at 298 K (crude).



b)



c)

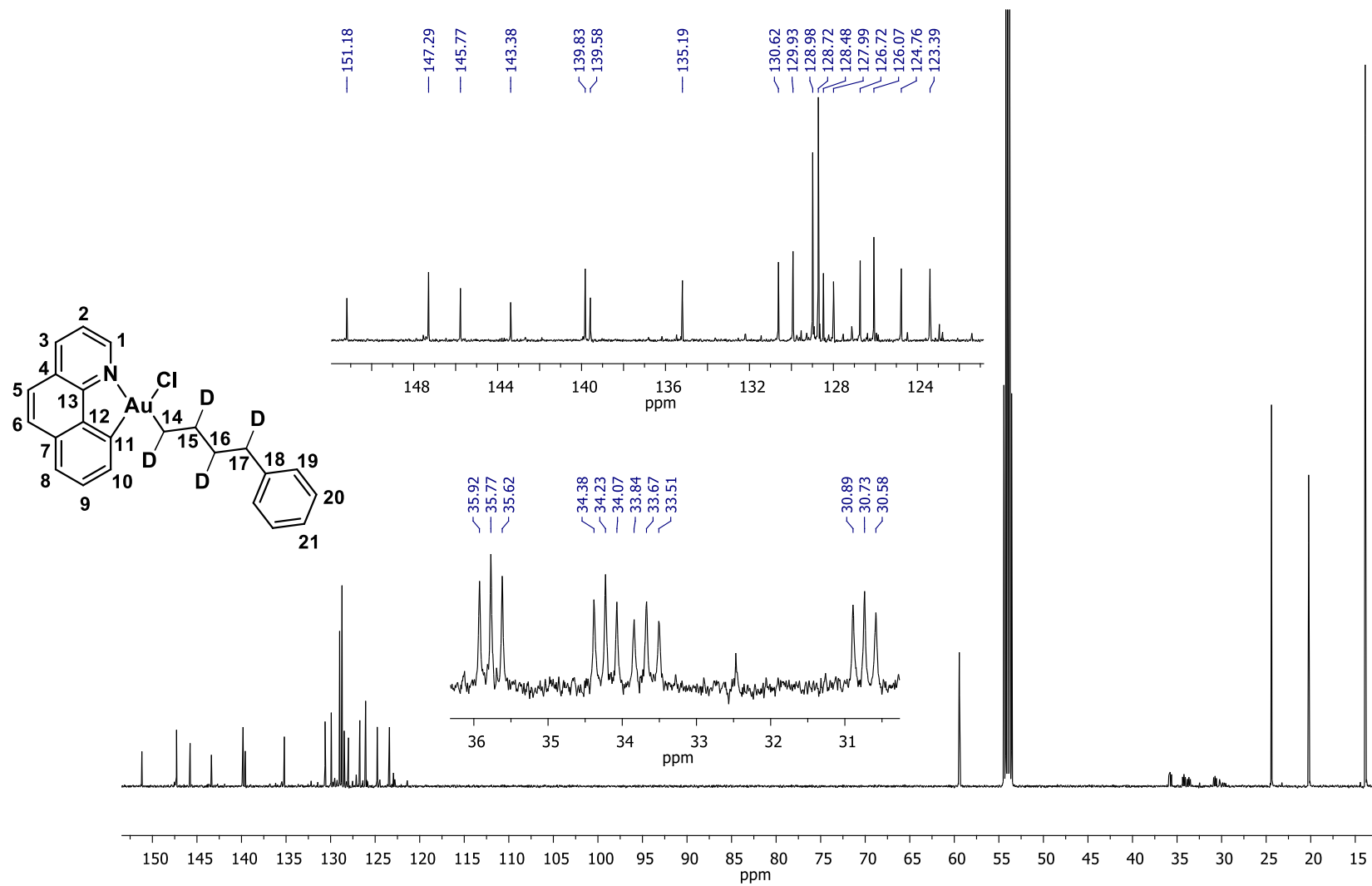
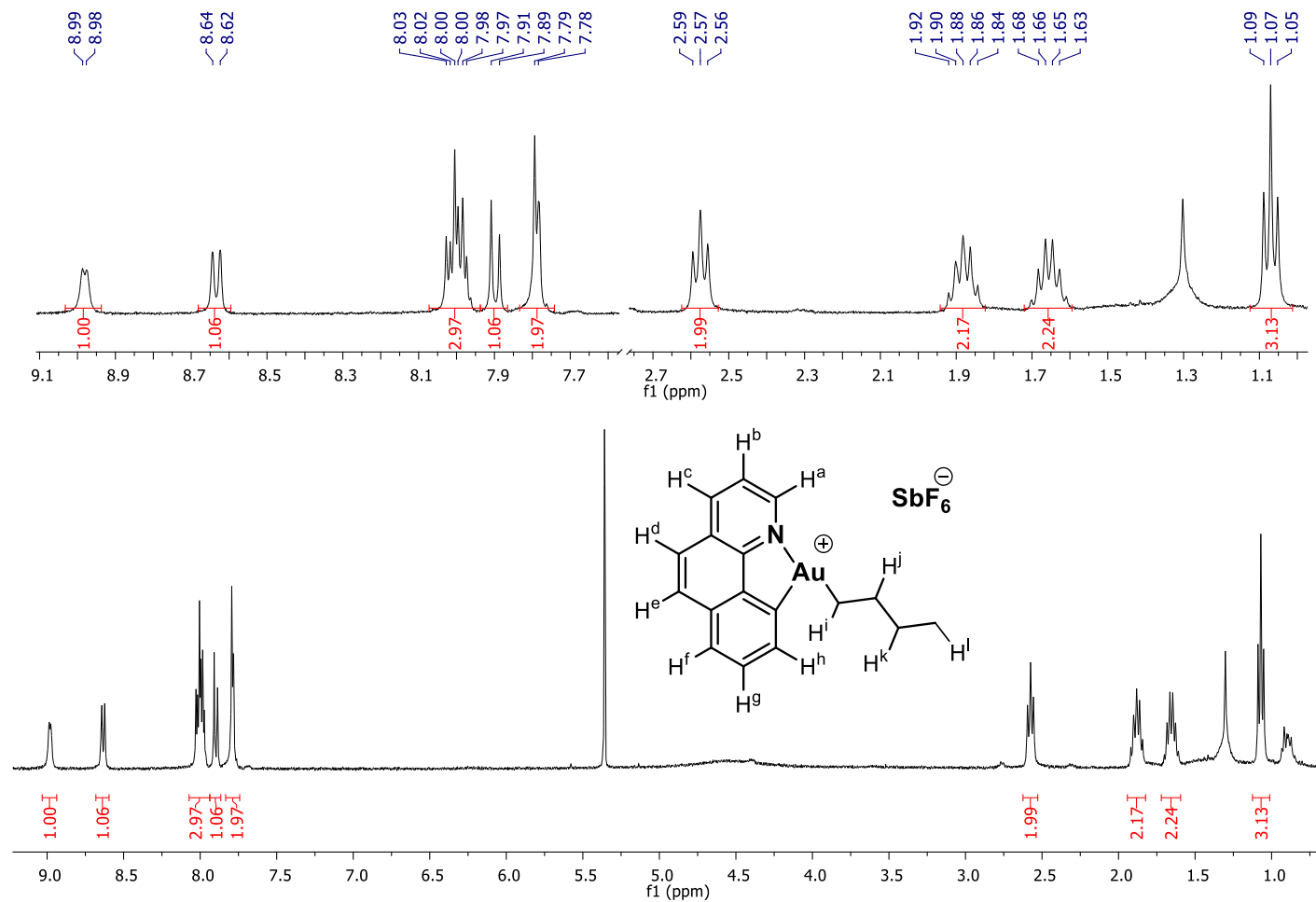


Figure S5. a) ^1H -NMR spectrum of complex **6A** in CD_2Cl_2 , 400 MHz, at 298 K; b) $^{13}\text{C}\{^1\text{H}\}$ -NMR spectrum (CD_2Cl_2 , 100 MHz, 298 K).

a)



b)

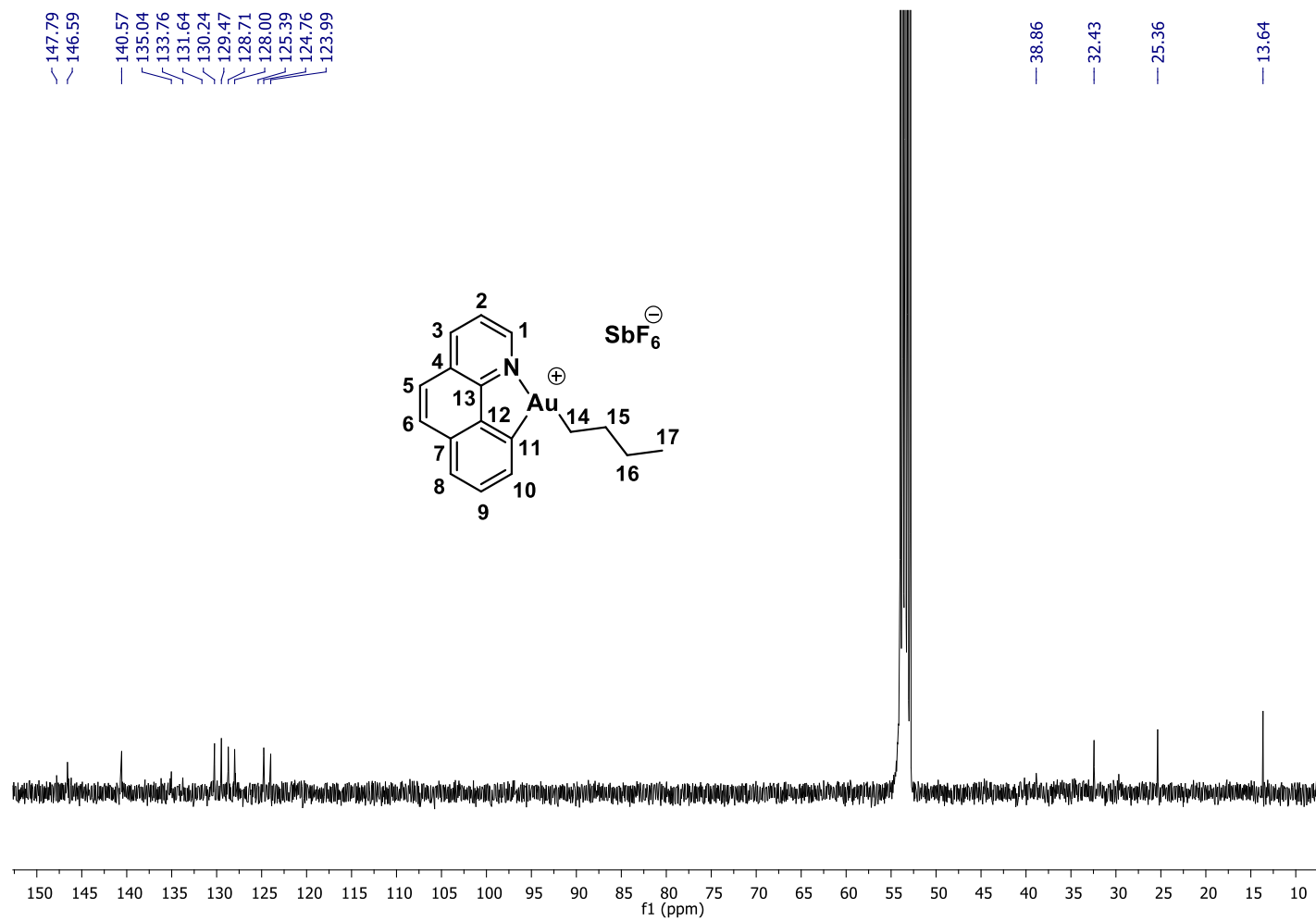
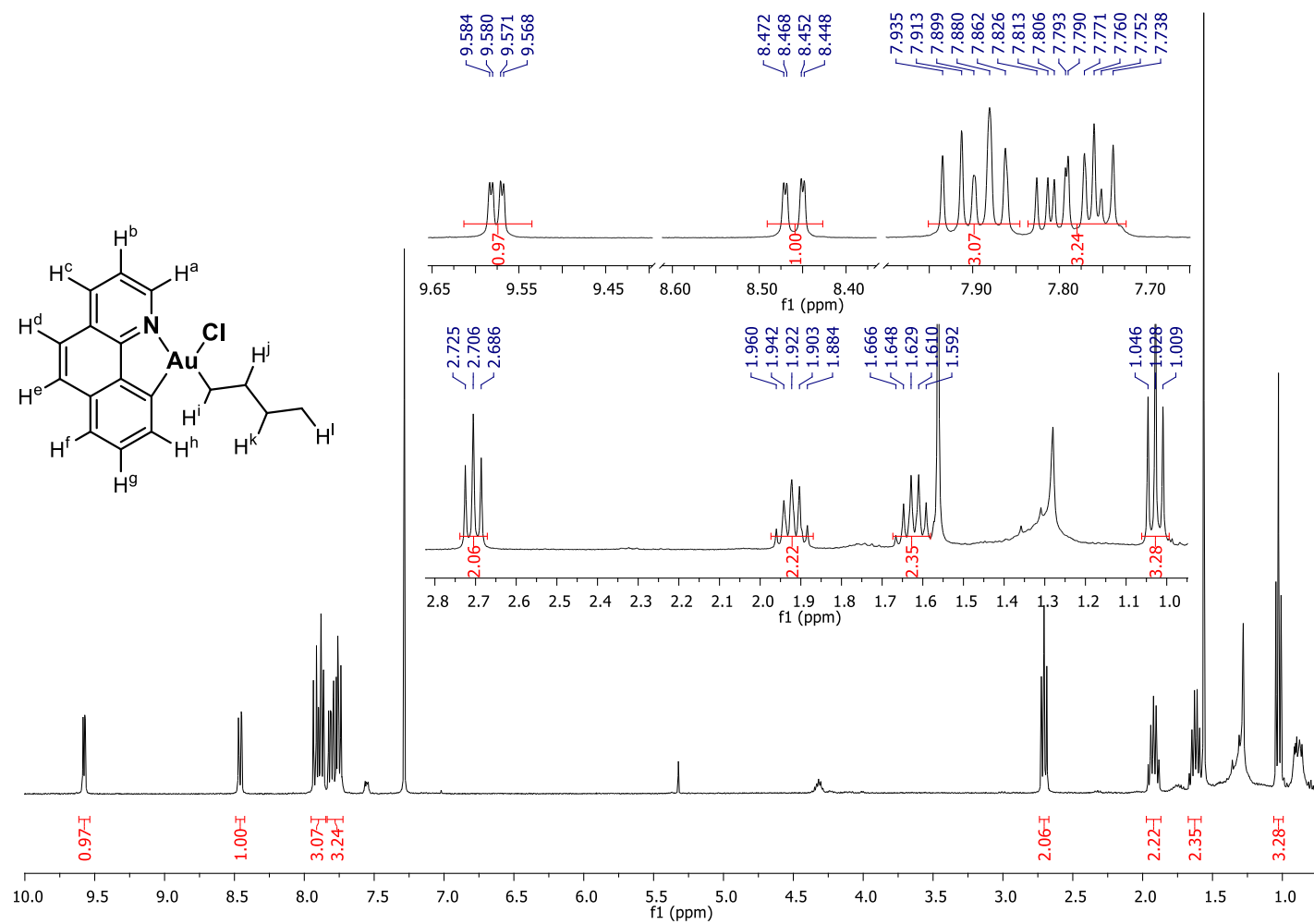


Figure S6. a) ^1H -NMR spectrum of complex **6-Cl** in CDCl_3 , 400 MHz, at 298 K; b) $^{13}\text{C}\{^1\text{H}\}$ -NMR spectrum (CDCl_3 , 100 MHz, 298 K).

a)



b)

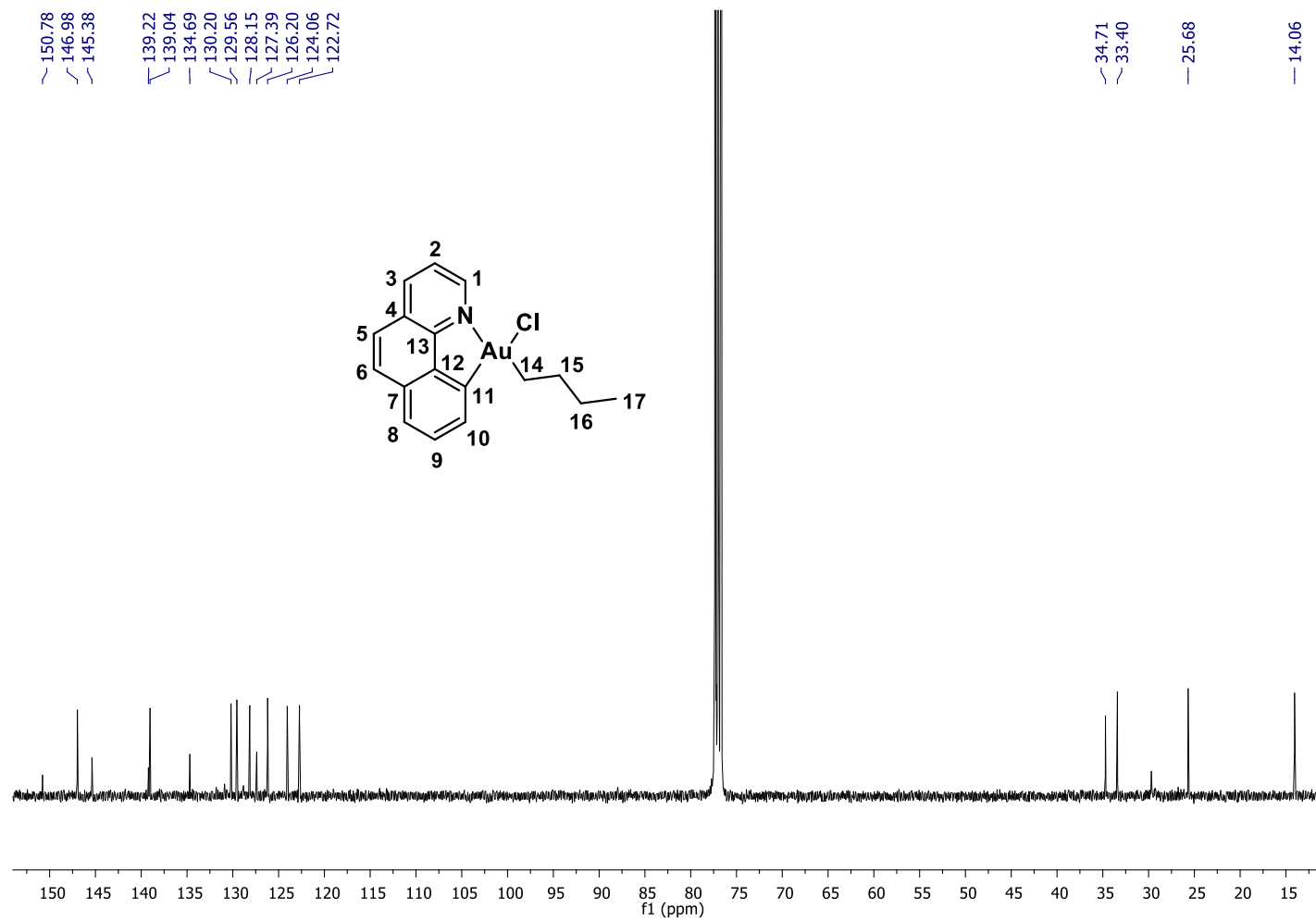


Figure S7. Full energy profile (ΔG and ΔE values into brackets, in kcal/mol) computed at the PCM(Dichloromethane)-B3PW91/SDD+f(Au)/6-31G** (other atoms) level of theory for different insertions of ethylene and β -hydride elimination from the [(N,C)AuPh]⁺ complex **1A** (*cis* and *trans* isomers).

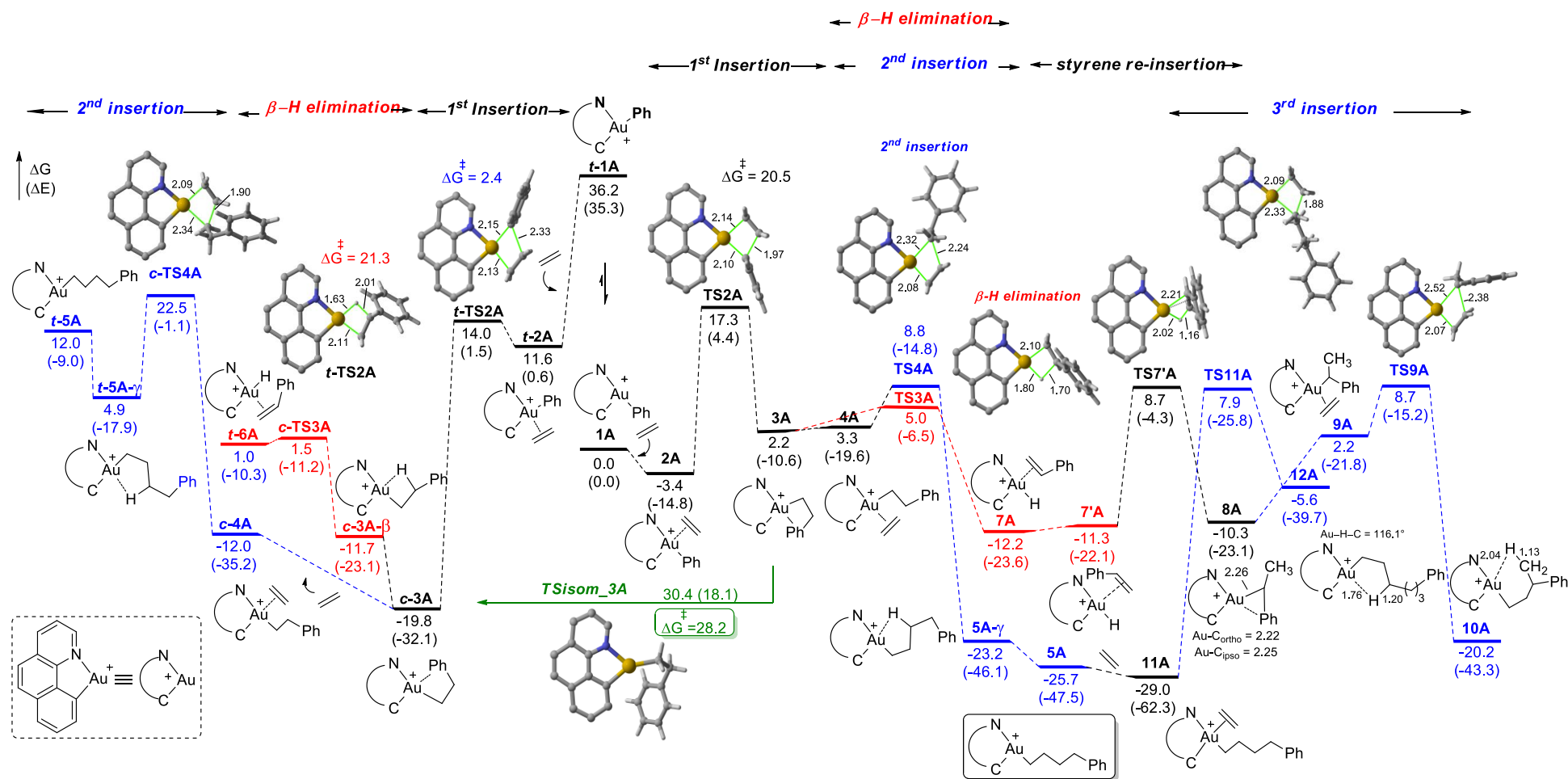


Figure S8. Key structures and selected geometric parameters (distances in Å) for the insertion of ethylene into the Au-Ph bond of complex **1A** at the PCM(Dichloromethane)-B3PW91/SDD+f(Au)/6-31G**(other atoms) level of theory.

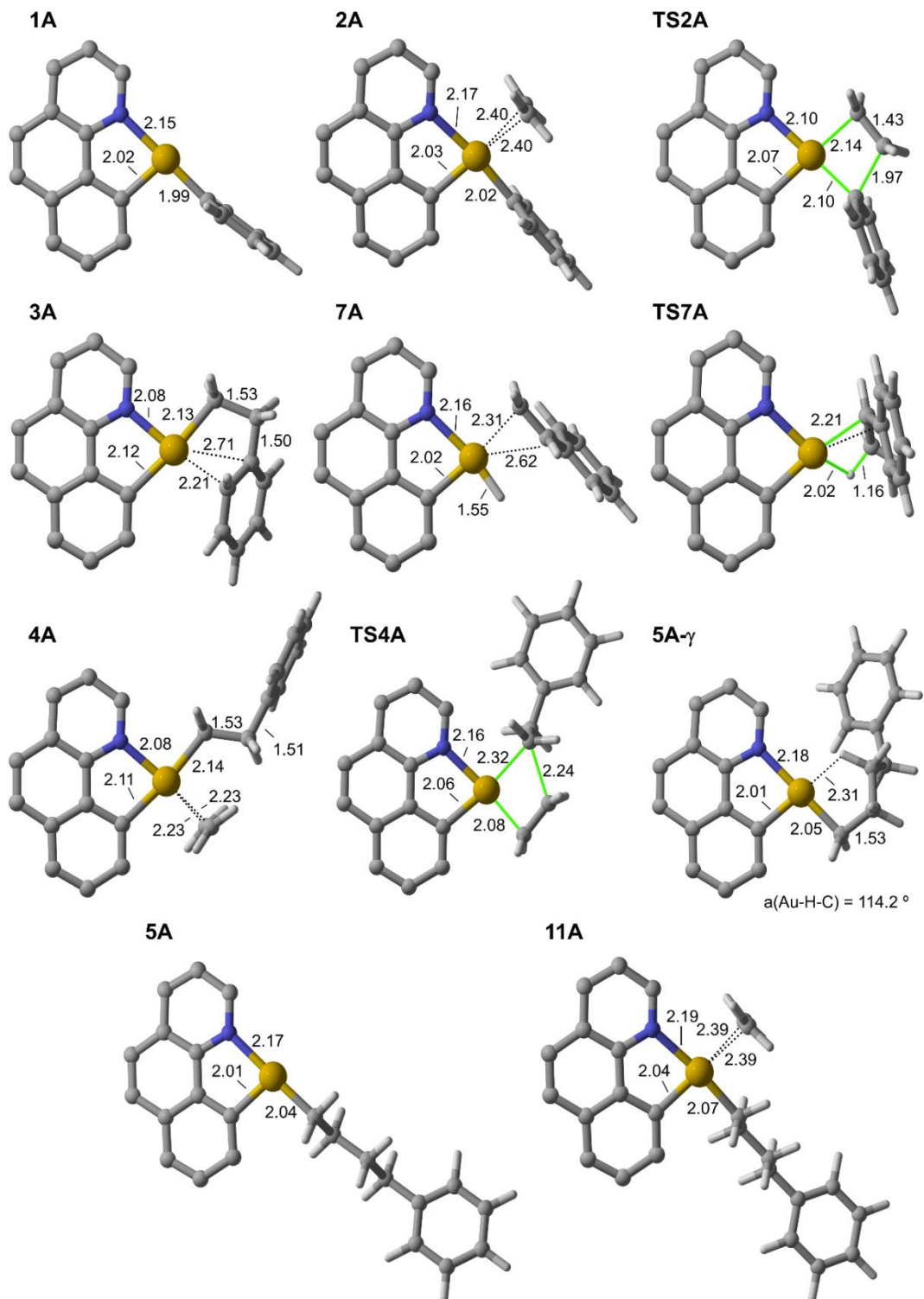
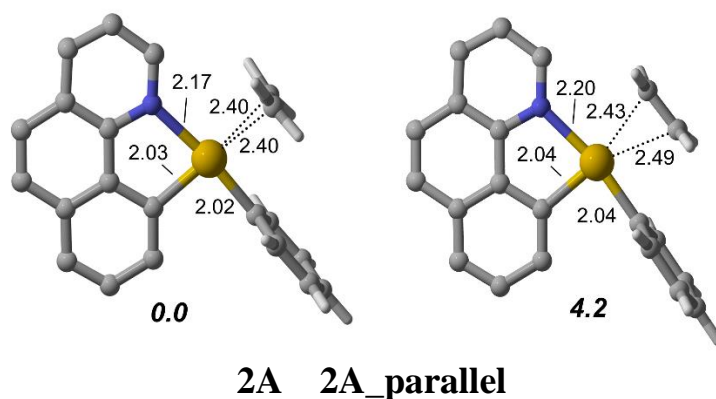


Table S1. NBO analysis of the π -ethylene coordination in complex **2A**, of the π -arene coordination in complex **3A** and of the γ -CH agostic interaction in complex **5A- γ** at the PCM(Dichloromethane)-B3PW91/SDD+f(Au)/6-31G**(other atoms) level of theory. Relative stability of complexes **2A** and **2A_parallel** in kcal/mol.



Complex	Donation ^a	Back-Donation ^a	NLMO ^b
2A <i>ethylene perpendicular</i>	45.7 ($\pi_{CC} \rightarrow \sigma^*_{AuC}$)	14.1 ($d_{Au} \rightarrow \pi^*_{CC}$)	43.7 % C 43.7 % C 6.5% Au 5.6% C _{naph}
2A_parallel <i>ethylene parallel</i>	50.9 ($\pi_{CC} \rightarrow \sigma^*_{AuC}$)	9.7 ($d_{Au} \rightarrow \pi^*_{CC}$)	40.2 % C 48.1% C 6.0 % Au 5.0 % % C _{naph}
3A	31.0 ($\pi_{CC} \rightarrow \sigma^*_{AuN}$)	-- ($d_{Au} \rightarrow \pi^*_{CC}$)	22.8 % C _{ipso} 50.5 % C _{ortho} 1.5% N 13.0% Au
5A-γ	7.1 ($\sigma_{CH} \rightarrow \sigma^*_{AuC}$)	2.3 ($\sigma_{AuC} \rightarrow \sigma^*_{C-H}$)	57.0 % C 40.2 % H 1.1 % Au

^a Stabilizing energy $\Delta E(2)$ in kcal/mol. ^b Participation of each atom (%) in the NLMO $\pi_{C=C}$ and the NLMO σ_{CH} .

Figure S9. Energy profiles (ΔG and ΔE values into brackets, in kcal/mol) computed at the PCM(Dichloromethane)-B3PW91/SDD+f(Au)/6-31G**(other atoms) level of theory for the third ethylene insertion from **5A** and second ethylene insertion from **8A**(see complete profile in Figure S13).

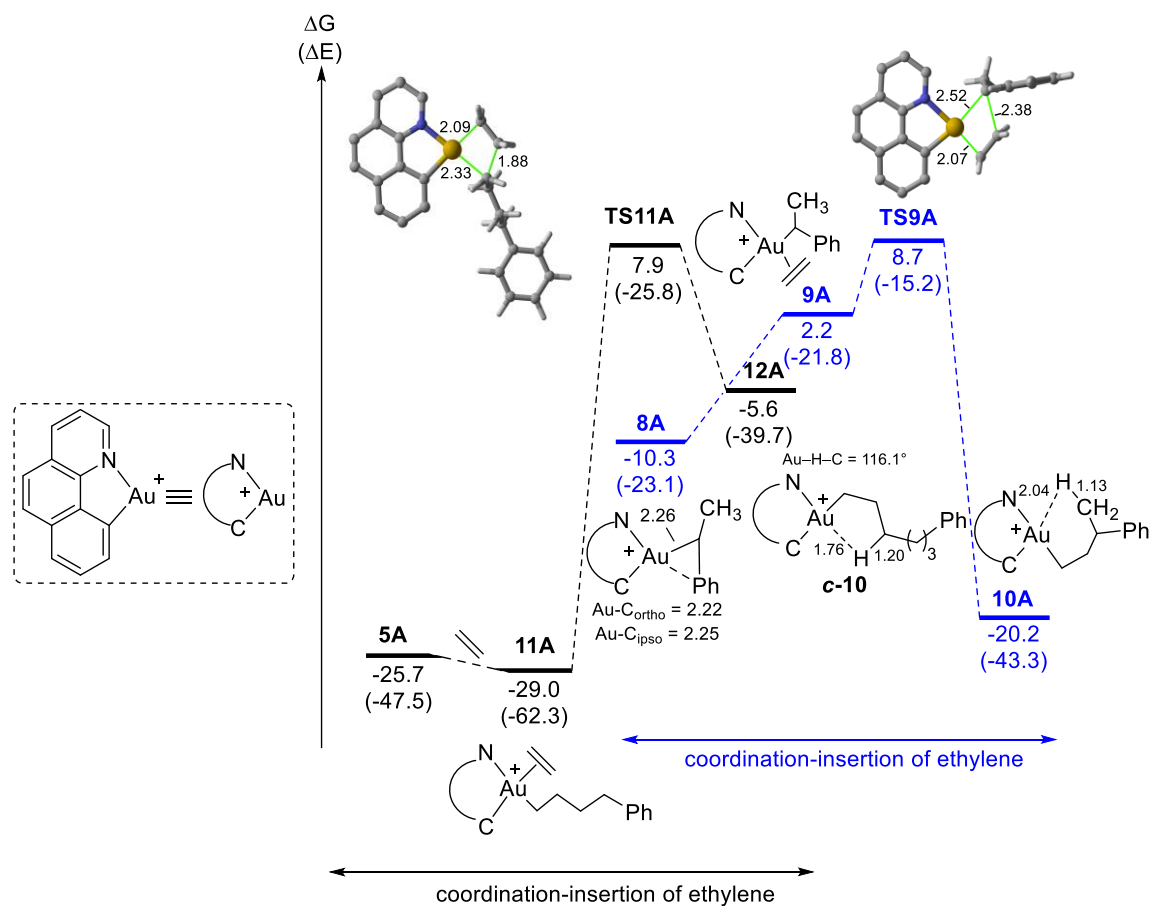


Figure S10. Energy profiles (ΔG and ΔE values into brackets, in kcal/mol) computed at the PCM(Dichloromethane)-B3PW91/SDD+f(Au)/6-31G**(other atoms) level of theory for β - and γ -hydride eliminations from complex **5A**.

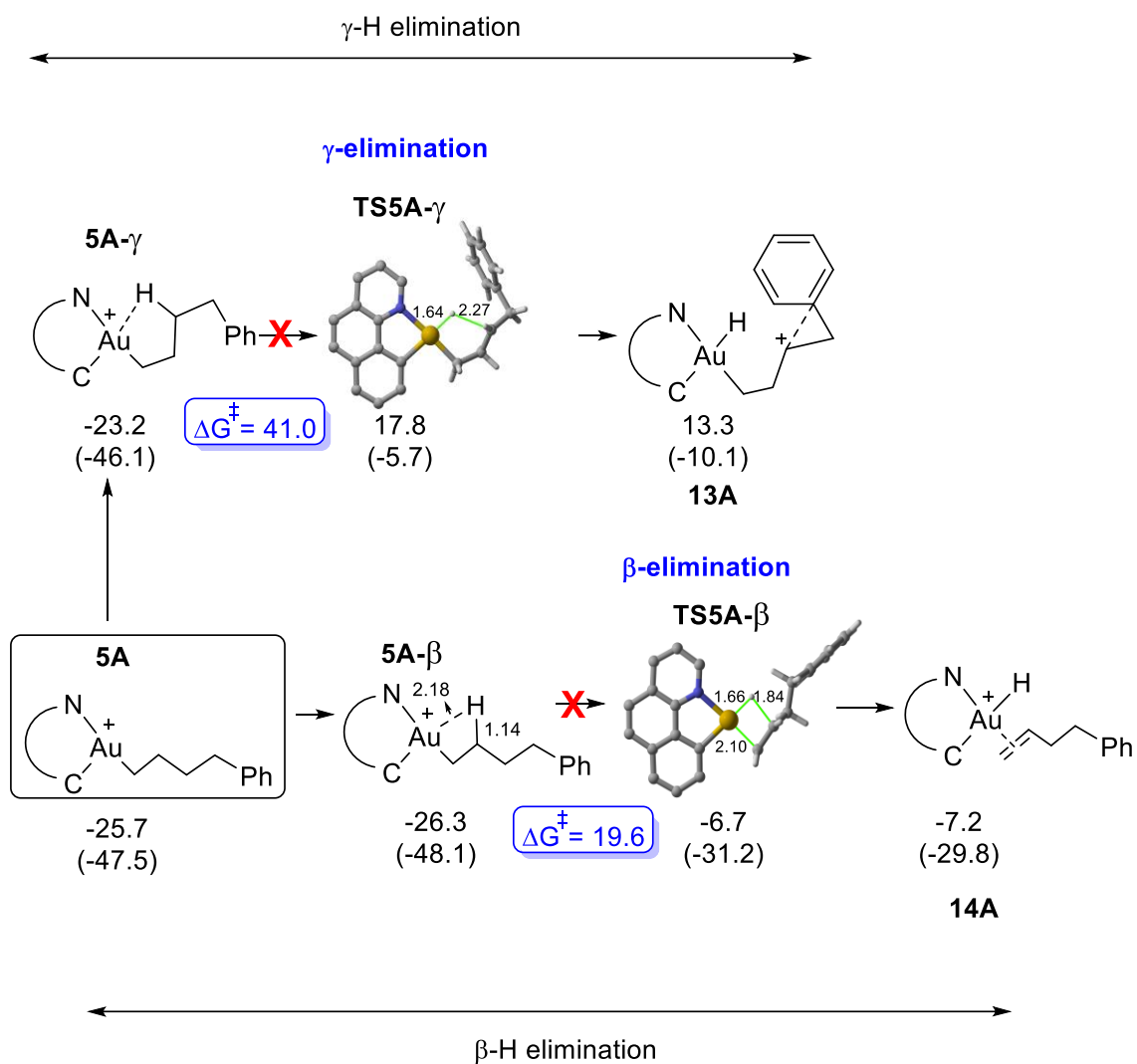


Figure S11. Energy profile (ΔG and ΔE values in kcal/mol) computed at the PCM(Dichloromethane)-B3PW91/SDD+f(Au)/6-31G**(other atoms) level of theory for β -hydride and 2nd insertion from *t*-3A (see complete profile in Figure S13).

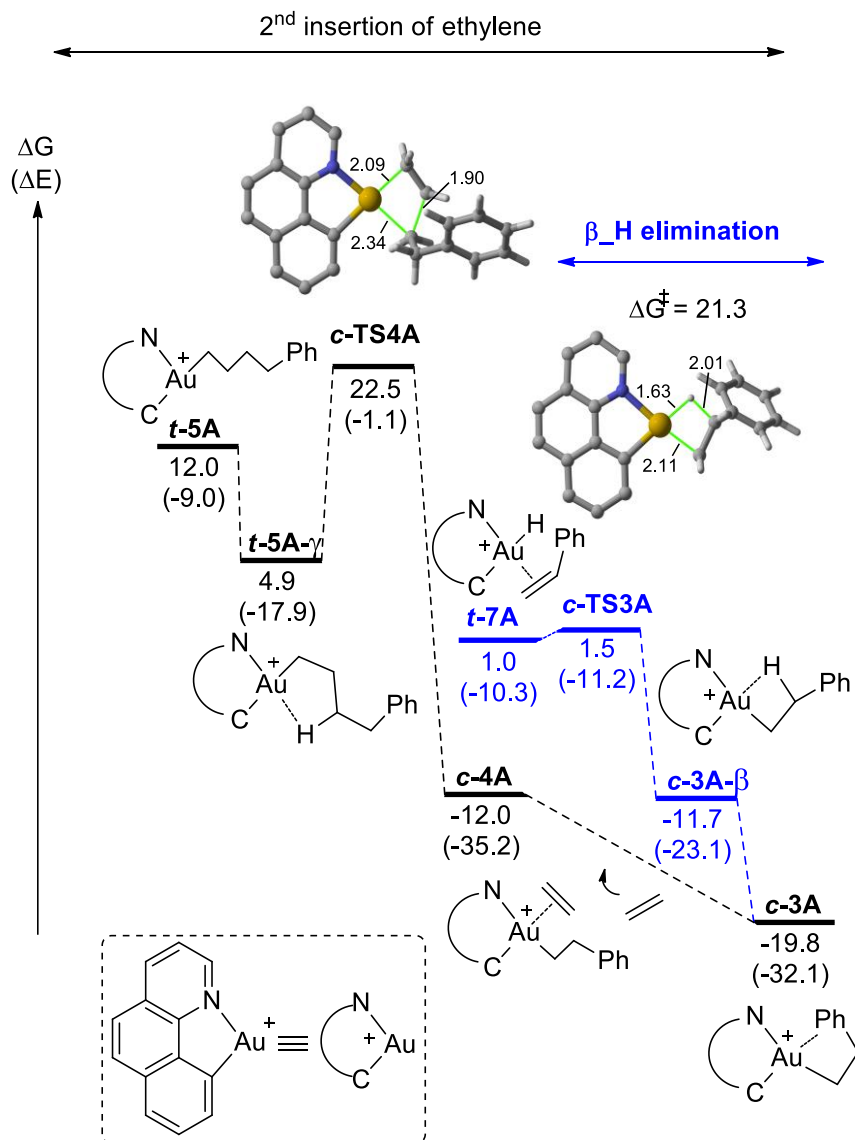


Figure S12. Energy profile (ΔG and ΔE values in kcal/mol) computed at the PCM(Dichloromethane)-B3PW91/SDD+f(Au)/6-31G**(other atoms) level of theory for ethylene insertion and β -hydride elimination from the [(P,C)AuPh]⁺ complex **1C**.

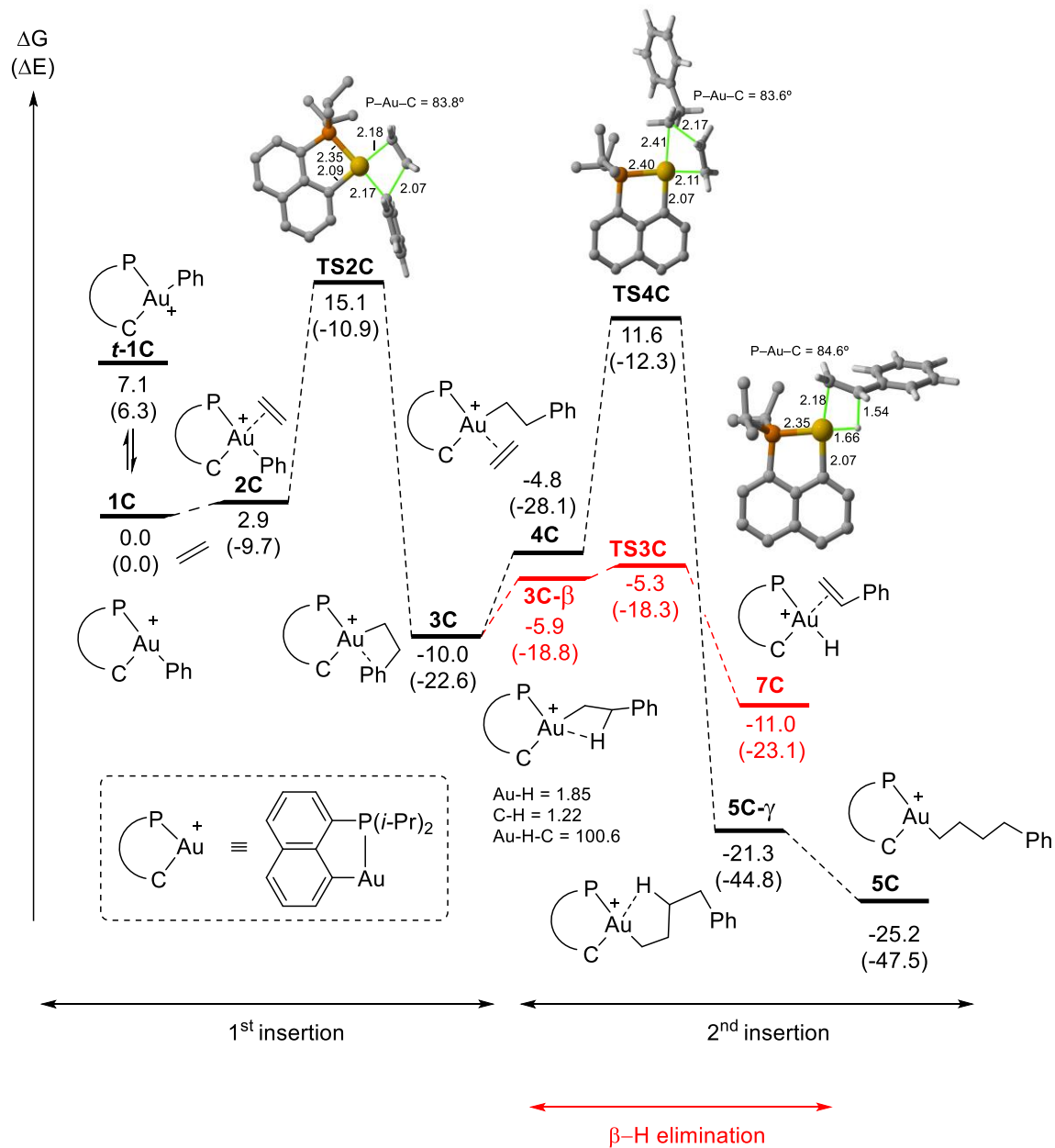


Figure S13. Key structures and selected geometric parameters (distances in Å) for the two first insertions of ethylene into the Au-Ph bond of complex **1C** and β -hydride elimination from **3C** at the PCM(Dichloromethane)-B3PW91/SDD+f(Au)/6-31G**(other atoms) level of theory.

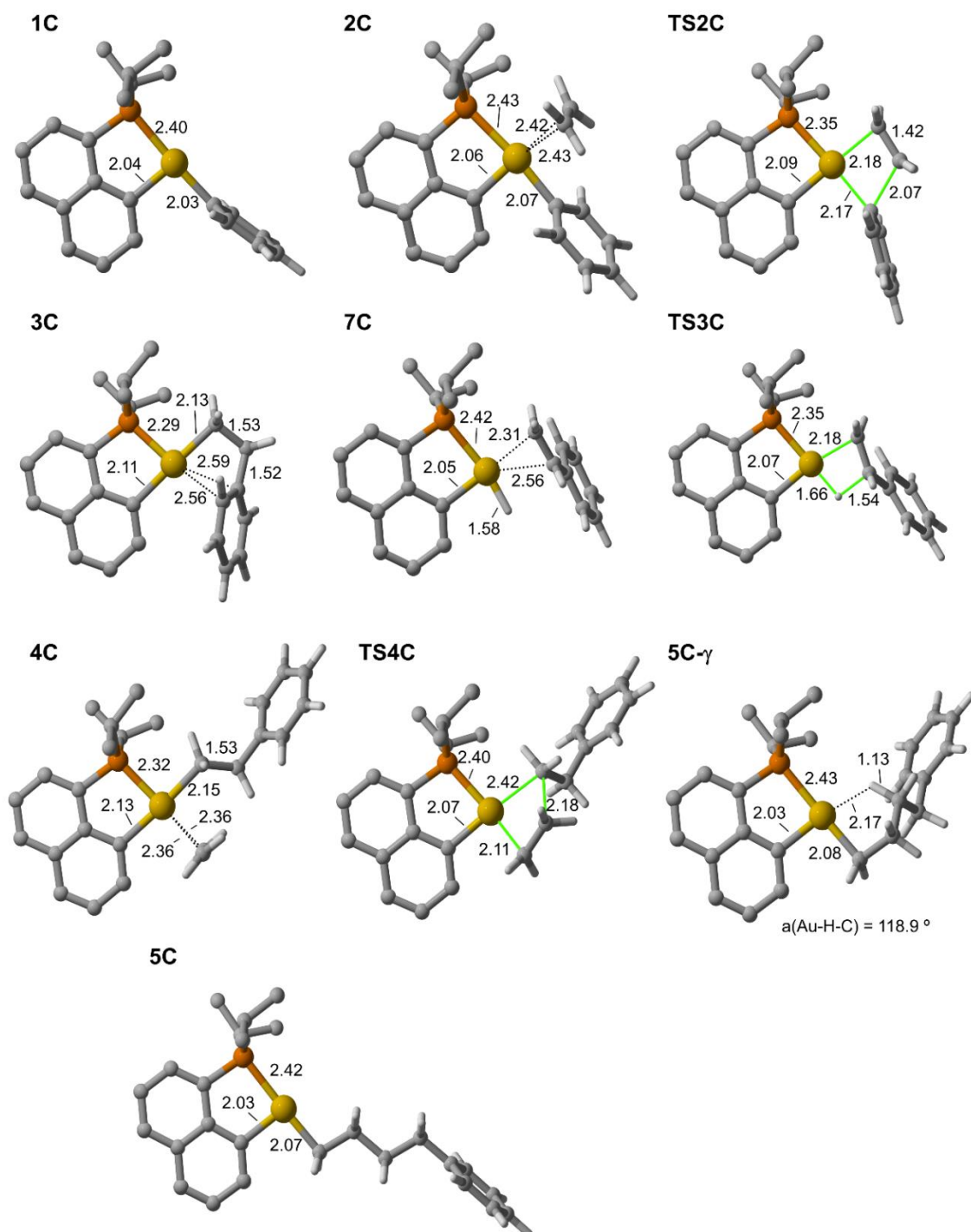


Figure S14. Reaction paths (ΔG and ΔE values, into brackets in kcal/mol) computed at the PCM(Dichloromethane)-B3PW91/SDD+f(Au)/6-31G**(other atoms) level of theory for the reductive elimination (C_{sp^2} -H coupling) of the gold(III) hydride complexes **7A** and **7C**.

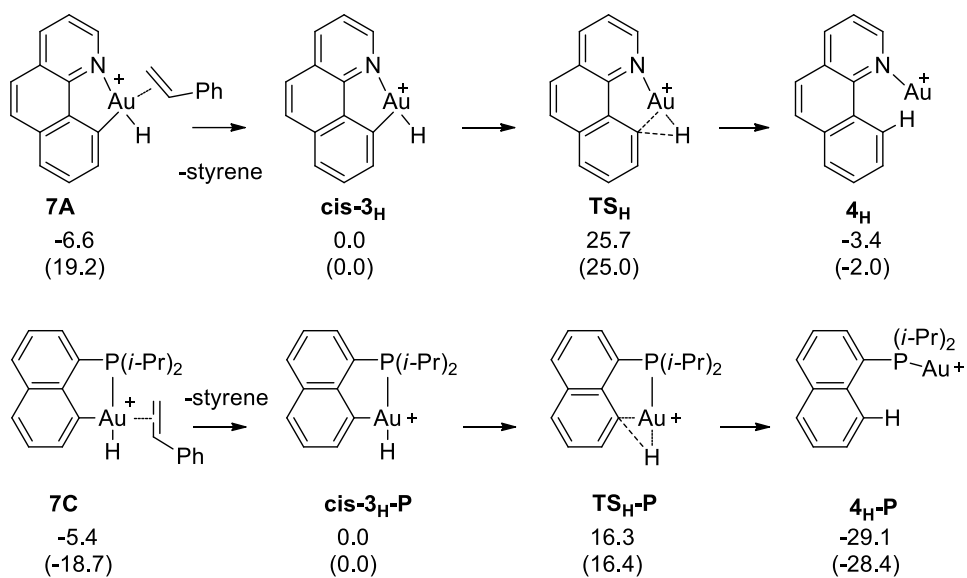
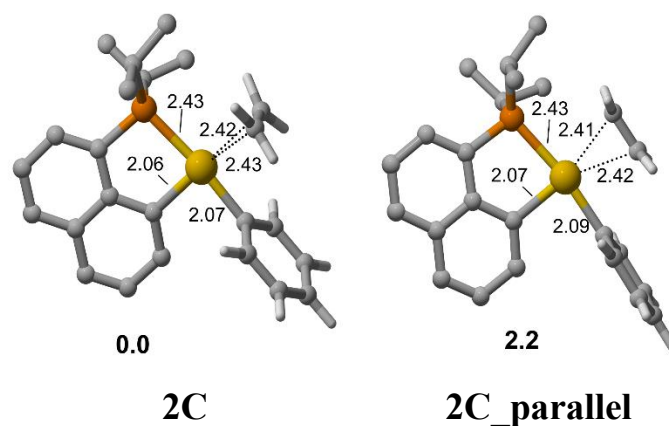


Table S2. NBO analysis of the π -ethylene coordination in complex **2C**, of the π -arene coordination in complex **3C** and of the γ -CH agostic interaction in complex **5C- γ** at the PCM(Dichloromethane)-B3PW91/SDD+f(Au)/6-31G**(other atoms) level of theory. Relative stability of complexes **2C** and **2C_parallel** in kcal/mol.



Complex	Donation	Back-Donation	NLMO
2C <i>ethylene perpendicular</i>	34.3 ($\pi_{CC} \rightarrow \sigma^*_{AuC}$)	13.0 ($d_{Au} \rightarrow \pi^*_{CC}$)	42.4 % C 44.2 % C 6.6 % Au 5.9 % C _{napht}
2C_parallel <i>ethylene parallel</i>	34.3 ($\pi_{CC} \rightarrow \sigma^*_{AuC}$) parallel	12.5 ($d_{Au} \rightarrow \pi^*_{CC}$)	40.2 % C 45.7 % C 6.9 % Au 6.2 % C _{napht}
3C	6.4 ($\pi_{CC} \rightarrow \sigma^*_{AuP}$)	4.0 ($d_{Au} \rightarrow \pi^*_{CC}$)	37.2 % C _{ipso} 42.4 % C _{ortho} 4.5 % Au 3.4 % P
5C-γ	2.2	12.0 ($\sigma_{C-H} \rightarrow \sigma^*_{AuC}$)	55.6 % C 40.5 % H 1.5 % Au

4. X-ray Crystallography Data

Crystallographic data for complexes **5A-H₂O** (CCDC-1574199) and **5A-Cl** (CCDC-1574200) can be obtained free of charge from the Cambridge Crystallographic Data Centre (CCDC) via www.ccdc.cam.ac.uk/data_request/cif.

Colorless crystals were grown from a CD₂Cl₂ solution of the compound for **5A-H₂O**, and from slow diffusion of pentane in a CHCl₃ solution of the **5A-Cl** complex. The data were collected at low temperature (193(2)K) on a Bruker-AXS APEX II QUAZAR diffractometer equipped with a 30W air-cooled microfocus source for **5A-H₂O** and on a Bruker-AXS PHOTON100 D8 VENTURE diffractometer for **5A-Cl**, using MoK α radiation ($\lambda = 0.71073 \text{ \AA}$). Phi- and omega-scans were used. An empirical absorption correction with SADABS was applied.^[17] The structures were solved by direct methods (SHELXS-97)^[18] or using Intrinsic phasing method (SHELXT)^[19] and refined by full-matrix least squares on F^2 .^[17] All non-H atoms were refined with anisotropic displacement parameters.

¹⁷SADABS. Bruker AXS Inc., Madison, Wisconsin, USA.

¹⁸ Sheldrick, G. M., *Acta Cryst.* **2008**, A64, 112-122.

¹⁹ Sheldrick, G. M., *Acta Cryst.* **2015**, A71, 3-8.

Table S3. Key structural parameters of complex **5A-H₂O**.

Chemical formula	C ₂₃ H ₂₃ Au ₁ N ₁ O ₁ ¹⁺ ,F ₆ Sb ₁ ¹⁻
fw (g mol⁻¹)	762.15
Bond precision	C-C = 0.0083 Å
T (K)	193
a (Å)	6.6287(3)
b (Å)	16.4246(8)
c (Å)	21.5858(11)
α (deg.)	90
β (deg.)	90
γ (deg.)	90
V (Å³)	2350.1(2)
ρ_{calcd.} (g cm⁻³)	2.154
λ (Å)	0.71073
Mu (mm-1)	7.448
F000	1440.0
F000'	1430.69
h,k,lmax	9,22,29
Nref	6595[3740]
R₁ [I>2σ(I)]	0.0262(6022)
wR₂ [I>2σ(I)]	0.0466(6582)

Figure S15. X-Ray structure of complex **5A-H₂O** obtained by crystallization from CD₂Cl₂. Ellipsoids are set at 50% probability.

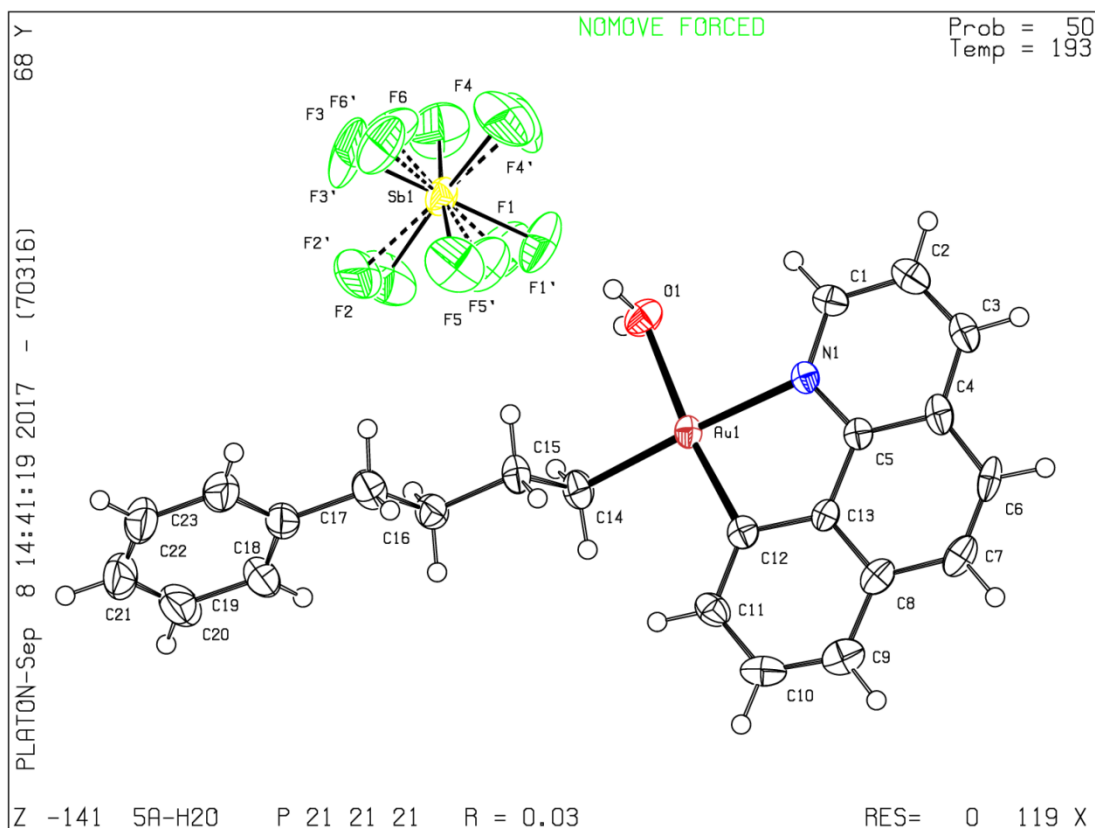


Table S4. Key structural parameters of complex **5A-Cl**.

Chemical formula	$C_{23}H_{21}Au_1Cl_1N_1C_1H_1Cl_3$
fw (g mol⁻¹)	663.20
Bond precision	C-C = 0.0055Å
T (K)	193
a (Å)	7.4651(4)
b (Å)	9.8244(5)
c (Å)	16.9630(9)
α (deg.)	98.935(2)
β (deg.)	91.454(2)
γ (deg.)	106.868(2)
V (Å³)	1172.83(11)
ρ_{calcd.} (g cm⁻³)	1.878
λ (Å)	0.71073
Mu (mm⁻¹)	6.739
F000	640.0
F000'	637.48
h, k, lmax	10,13,23
Nref	6872
R₁ [I>2σ(I)]	0.0247(6265)
wR₂ [I>2σ(I)]	0.0583(6865)

Figure S16. X-Ray structure of complex **5A-Cl** obtained by crystallization from CHCl₃. Ellipsoids are set at 50% probability.

